UNIVERSITA' DEGLI STUDI DI PAVIA

Dipartimento di Medicina Molecolare

The origin of unbalanced *de novo* chromosome translocations and inversions

Paolo Reho

Dottorato di Ricerca in
Genetica, Biologia Molecolare e Cellulare
XXIX Ciclo – A.A. 2013-2016

UNIVERSITA' DEGLI STUDI DI PAVIA

Dipartimento di Medicina Molecolare

The origin of unbalanced *de novo* chromosome translocations and inversions

Paolo Reho

Supervised by Prof. Orsetta Zuffardi

Dottorato di Ricerca in
Genetica, Biologia Molecolare e Cellulare
XXIX Ciclo – A.A. 2013-2016

Abstract

The origin of de novo unbalanced translocations and unbalanced rearrangements mimicking a derivative from a pericentric inversion (herein called unbalanced inversions) is still enigmatic.

We studied 43 of these *de novo* unbalanced rearrangements, two of them with more than one cell line, as detected in blood, including simple translocations (n=29), inv-dup del translocations (n=7), inversions (n=6), and inv-dup del inversions (n=1) in order to highlight their parental origin and mechanisms of formation.

We also sequenced 19 breakpoint junctions between the derivative chromosome and the translocated portion of another chromosome or the same chromosome and detected a number of different motifs: 2 to 6 base pairs microhomologies (n=8), short insertions of 1 to 36 base pairs (n=8), LINE/L1-mediated non-allelic homologous recombination (n=2) and fork stalling and template switching (n=1).

Parental origin was fully informative in 27 out of 43 cases, informative for only one imbalance (6 paternal and 3 maternal) in 9 cases, while in the remaining 8 cases no information was available.

While all unbalanced inversions were of paternal origin, most simple translocations were of maternal origin (n=15), and two displayed bi-parental origin, showing that they originated post-zygotically. Only in one unbalanced translocation the duplicated portion showed three alleles, two of them of maternal origin, indicating that the zygote was possibly trisomic for that chromosome, as effect of maternal meiosis I non-disjunction.

Thus, the translocation reflects the partial rescue by telomere capture of the supernumerary chromosome. This hypothesis is also supported by one case with three cell lines: a minor one with trisomy 9, a second line with unbalanced translocation t(9;14), and a third with normal karyotype.

The inv-dup del translocations/inversions are likely the result of an original dicentric chromosome that after its breakage was stabilized by telomere capture

Our findings suggest that partial rescue, through single- or multiple-step mechanisms, of an abnormal zygotic chromosome complement, consisting of either (i) a rearranged chromosome, such as a terminally deleted or dicentric "mirror" chromosome, or (ii) a whole supernumerary chromosome is the most likely mechanism leading to *de novo* unbalanced translocations/inversions.

Accordingly, these de novo rearrangements do not imply any risk of recurrence in subsequent pregnancies.

Acknowledgements

Patients and their families described in this research study are deeply acknowledged. The Ring14 International Society and Dr Chiara Baldo from the Galliera Genetic Bank, Laboratory of Human Genetics, EO Ospedale Galliera, Genova, Italy provided material from case 26. The Telethon Italian Foundation (Grant GGP13060) to my tutor, Orsetta Zuffardi contributed to support this study.

Contents

1. Introduction

Translocations are among the most common structural chromosome abnormalities found in humans. They are classified into balanced (or reciprocal), and unbalanced rearrangements, the latter being characterized, in most of the cases, by a regular number of 46 with one chromosome partially deleted at one of its distal p or q region to which the terminal p or q portion of another chromosome is attached. The latter condition results in variable and sometime lethal phenotypic disorders as a consequence of the monosomy for a chromosomal region and the duplication for another one. The frequency of this type of rearrangements has been estimated using conventional cytogenetics to be 0.02% in unselected newborns (Jacobs PA et al. 1992) and 0.7-1.1% in individuals with developmental disabilities (Ravnan JB et al. 2006; Shao L et al. 2008). In 22% of prenatally detected cases, mainly ascertained because of advanced maternal age or ultrasound findings (Chang YW et al. 2013), and 30% among subjects with developmental delay (Robberecht C et al. 2013), the unbalanced translocation was demonstrated to be arisen de novo. In contrast, constitutional balanced translocations (1 in 500 people) do not have phenotypic consequences in about 94% of the *de novo* cases (Warburton D 1991). The rearrangement may even be passed down through the generations, without being identified until a carrier has repeated miscarriages or has a child affected by congenital malformation/intellectual disability due to any of the possible unbalanced segregations of the translocation at gametogenesis. Carrier males may also present infertility by reduction of sperm production, showing in most of the cases moderate-to-severe oligoasthenospermia for autosome;autosome

translocations and azoospemia for X;autosome or Y;autosome translocations (Gao M et al. 2016).

The remaining 6% of subjects carrying a de novo apparently balanced translocation presents with intellectual disabilities and/or congenital defects. It has been demonstrated that in these cases, either the translocation, although reciprocal, is not balanced (De Gregori M et al. 2007) hiding cryptic deletions at one or both breakpoints, or having one of the breakpoints that interrupts a dosage-sensitive gene or its cis-acting elements. In the latter cases, the proper transcription of one or more than one gene may be impaired. A different situation is documented for acquired balanced chromosome translocations that are common pathogenetic events in cancer. In contrast to the constitutional translocations that are in most cases private events, belonging to that person/family, cancer translocations are recurrent events in most tumors, thus being among the most valuable determinants of diagnosis and prognosis. The mechanisms promoting the occurrence of a de novo translocation, either constitutional or acquired, are poorly understood. For the constitutional ones, at least two translocations are recurrent in the population, namely the t(11;22)(q23;q11), the most common recurring reciprocal translocation seen in humans, and the t(4;8)(p16.1;p23.1).

The t(11;22) translocation is mediated by potentially cruciform-forming sequences at the breakpoints of both chromosomes, characterized by palindromic AT-rich repeats (PATRRs) which do not share sequence homology with one another. The majority of the breakpoints are located at the center of the PATRRs, suggesting that genomic instability of the palindrome center is the etiology of the recurrent translocation (Kato T et al. 2011). The t(4;8) translocation results from exchange between two clusters

of olfactory-receptor genes on 4p and 8p via homologous recombination (Giglio S et al. 2001). For the nonrecurrent constitutional balanced translocations, DNA double-strand breaks (DSBs) are presumably common intermediates although a clear picture of the mechanisms leading to the rearrangement is still missing.

The origin of de novo unbalanced translocations is even more enigmatic. The possibility that the imbalance is due to unbalanced segregation of a balanced rearrangement present in mosaic in one of the parents, does not appear likely. In fact, in this case, more siblings having the de novo unbalanced translocation should have been detected at least in some cases, what in fact is not documented.

Regarding inversions, consisting in a single chromosome showing a 180-degree reversal orientation of a part of it, their frequency ranges from about 0.012% to 0.07% (pericentric) and about 0.01% to 0.05% (paracentric) of individuals as estimated by conventional cytogenetics (Van Dyke DL et al. 1983; Kleczkowska A et al. 1987; Worsham MJ et al. 1989; Pettenati MJ et al. 1995). In the last 15 years, FISH and massive sequencing showed that the frequency of cryptic paracentric inversion is much higher. As previously suspected (Madan,1995), most of them have been demonstrated to be polymorphisms with different frequency in the different populations and represent risk factors increasing the occurrence of an unbalanced causative rearrangements (Antonacci F et al. 2009). Among subjects with congenital malformations/intellectual disability, conventional and molecular chromosome investigations highlighted some with the duplication of the distal p or q segment and deletion of the opposite one. Some of them are the derivative product of a parental pericentric inversion, while some resulted to

be a *de novo* event. The frequency of both these types of rearrangements is unknown and the mechanisms leading to the de novo rearrangements mimicking recombinants from a parental pericentric inversion is enigmatic (Rivera H et al. 2013).

Altogether, several studies highlighted the importance of Alu and LINE repetitive elements as substrates for different types of rearrangements. In fact, Roberrecht and colleagues analysed 12 cases of *de novo* unbalanced translocations and identified non-allelic homologous recombination, particularly between long interspersed elements, as the predominant mechanism of *de novo* unbalanced translocations formation (Roberrecht C et al. 2013).

In contrast, Weckselblatt groups investigated the breakpoints signature in 57 unbalanced translocations and demonstrated that they do not arise primarily from NAHR but rather by non-homologous end-joining (NHEJ) or microhomology-mediated break induced replication (MMBIR) (Weckselblatt B et al. 2015).

Furthermore NAHR, NHEJ and telomere transposition have been invoked in the genesis of *de novo* simple unbalanced inversions (Rivera et al.2013).

The initial exchange of genetic material between two non-homologous chromosomes can occur during premeiotic mitoses, meiotic recombination in the parental germline, or post-zygotic mitoses in the early embryo (Weckselblatt B et al. 2015). Roberrecht showed that in six out twelve of their cases the *de novo* simple unbalanced translocations originated at meiosis I, three of them showed a post-zygotic events, and three could have either a postzygotic or a meiosis II origin (Roberrecht C et al. 2013).

These data show that, in spite of the common assumption that a germline *de novo* rearrangement present in all cells of the examined tissue originated in a parental germinal cell line, postzygotic events may play a role even in the formation of non-mosaic *de novo* unbalanced translocation where the deleted and the duplicated chromosome have bi-parental origin (Giorda R et al, 2008). Altogether, these findings clearly demonstrate how molecular investigations are changing our models on the origin of chromosome rearrangements.

We studied 43 *de novo* unbalanced rearrangements, divided in four different classes: class A) simple translocations (n=29), class B) inverted-duplication deletion translocations (n=7), class C) simple inversions (n=6), class D) inverted-duplication deletion inversions (n=1).

We systematically performed a molecular characterization (conventional karyotype, subtelomeric FISH and array-CGH analysis) and parental origin analysis of the deleted and duplicated segments in order to highlight their parental origin and acquire by the breakpoints signature which are their mechanisms of formation.

Parental origin analysis was informative in 27 cases, while in 9 cases we obtained information only for one imbalance and in 7 cases the analysis was not informative. Class C and D unbalanced inversions showed a paternal origin, most simple translocations were of maternal origin (n=15) but two of them displayed a bi-parental inheritance, highlighting their post-zygotic origin and in one of them the duplicated portion showed three alleles, indication of a maternal meiosis I non-disjunction.

Finally, breakpoint junction characterization was performed in 19 cases showing a series of different motifs: from 2 to 6 base pairs microhomologies (n=8), from 1 to 36 base pairs insertions (n=7), long interspersed elements mediated non allelic homologous recombination (N=2) and fork stalling and template switching (n=1).

Our findings suggest that *de novo* unbalanced translocations and inversions could originate, through single- or multiplestep mechanisms, from (1) terminal deletions stabilized by telomerase-independent mechanisms, such as telomere capture; (2) partial rescue of autosomal trisomies resulting from meiosis I non-disjunction; (3) dicentric chromosome formation and breakage, subsequently stabilized by telomere capture. Consequently, these *de novo* structural chromosome abnormalities do not involve any significant risk of recurrence in subsequent pregnancies.

2. Aims of the research

We studied 43 *de novo* unbalanced rearrangements, divided in four different classes: class A) simple translocations (n=29), class B) inverted-duplication deletion translocations (n=7), class C) simple inversions (n=6), class D) inverted-duplication deletion inversion s(n=1).

Cases of *de novo* deletions associated with apparently balanced translocations and cases of complex rearrangements involving more than two chromosomes were not taken into consideration.

We systematically performed a molecular characterization trhought conventional karyotype, FISH and array-CGH analysis, parental origin and breakpoint cloning of the deleted and duplicated segments, to detect specific breakpoints signatures clarifying the mechanisms and the time of formation of these types of rearrangements and to highlight any possible genomic polymorphism favouring their occurrence.

3. Materials and methods

Subjects

Blood samples were obtained from probands and their parents after informed consent. We collected 43 subjects showing a derivative chromosome ascertained through routine cytogenetic analysis (conventional karyotype, subtelomeric FISH or array-CGH analysis). Thirty-nine cases were ascertained because of intellectual disability/psychomotor delay, one (case 25) because of couple infertility, while three were prenatal cases (cases 12, 13 and 37) ascertained because of ultrasound abnormalities. The chromosomal imbalance was present in all cells except for cases 25 and 26 .

Molecular analysis

Probands' and parents' DNA was extracted from venous blood with standard protocols. Array-CGH analysis was performed in all patients using Array CGH Kits (G4411B, G4449A, Agilent Technologies, Santa Clara, CA) and 180K CGH+SNP array (G4890A, Agilent Technologies) following standard manufacturer protocols.

All nucleotide positions refer to the Human Genome, Feb 2009 Assembly (GRCh37, hg19). The array was analysed using an Agilent scanner and Feature Extraction V.9.1 software (Agilent Technologies). A graphical overview of the results was obtained using CGH Analytics V.3.4.27 and Cytogenomics software. SNP array was performed using the Human Omni Express Exome ILLUMINA v1.2 constituted by 964,193 SNP probes. SNPs

data analysis was performed using Illumina Genome Studio v.2011.1 software as well as Illumina CNV Partition (ver 2.3.4) and PennCNV software (version June 2011). Genotyping of polymorphic loci was performed by amplification with primers labeled with fluorescent probes (ABI 5-Fam, Hex and Tet) followed by analysis on a ABI 310 Genetic Analyzer (Applied Biosystems, Monza, Italy).

FISH analysis

FISH was performed on metaphase cells according to standard procedures. BAC clones were selected from the human RPCI-11 library according to the Human Genome Feb 2009 assembly (http://genome.ucsc.edu/cgi-bin/hgGateway) and provided by the BACPAC Resource Center (BPRC) at the Children's Hospital Oakland Research Institute in Oakland, CA (http://bacpac.chori.org/). BAC DNAs were labelled by either biotin-16-dUTP or digoxigenin using 27 a nick translation kit (Roche or Vysis). FISH with probes for all subtelomeric regions (TelVysion kit, VYSIS) were performed on selected cases. The pan-telomeric peptide nucleic acid (PNA) probe (PNA FISH kit/Cy3, Dako, Denmark), which recognizes the consensus sequence (TTAGGG)n of human pan-telomeres, was hybridized according to manufacturer's instructions. The chromosomes were counterstained with DAPI (Sigma Aldrich, St Louis, MO). Double-colour FISH was performed on the following Class B subjects: Case 30 with probes RP11-501G22 (AC007366: Xp22.33) and RP11-413F15 (AC073617 Xp22.32) labelled with biotin-16-dUTP and digoxigenin, respectively. Case 34 with probes RP11-399J23 (BZ089393: 8p 23.1) and RP11-589N15

(BZ089408: 8p23.1) labelled with labelled with biotin-16-dUTP and digoxigenin, respectively. The labelled probes were visualized with FITC-avidin (Vector, Burlingame, CA) or Rhodaminconjugated anti-digoxigenin (Sigma Aldrich, St Louis, MO). Hybridizations were analysed using an Olympus BX71 epifluorescence microscope and images captured with the Power Gene FISH System (PSI, Newcastle upon Tyne, UK).

Parental origin determination and breakpoint cloning

Mate-pair libraries were constructed using 1µg of DNA following the instruction for a gel-free preparation of 2 kb effective insert size library (Mate Pair Library v2, Illumina). Final libraries were quantified using Pico Green (Quant-iT, Invitrogen). Ten different indexed libraries were pooled together in a single flowcell and sequenced on a NextSeq (Illumina, San Diego, CA, USA) (2Å~75 bp). Raw sequence reads first were trimmed; cutadapt (Martin M 2011) was used to remove the adaptors. The remaining pairs passing Illumina Chastity filtering (>0.6) were mapped to the human reference genome (GRCh37/hg19) using Burrows Wheeler Aligner (BWA). To annotate the unique structural variations, reads not aligning uniquely were removed and the ones with unexpected orientation or aligning to different chromosomes were extracted using SVDetect (http://svdetect.sourceforge.net/) and Delly (www.korbel.embl.de/ software.html). Usually the predicted SVs are compared with multiple in-house mate-pair data sets to identify sample-specific SVs and all non-unique rearrangements, but for unbalanced translocations/inversions the estimated region detected by array CGH was also used to find the approximate

breakpoint regions. By uploading the BAM files (containing all the reads, both concordant and discordant) into Integrative Genomics Viewer (IGV) (Broad Institute, Cambridge, MA, USA) we were able to visualize the CNVs related to unbalanced translocation/inversion using depth of coverage of the aligned matepair and the cluster of reads that indicated the breakpoint regions. All cases were compared with at least two controls to identify potential deletions or duplications. Depending on the insert size and, in a few cases, split reads, mate-pair sequencing narrowed the breakpoint regions to 3kb-1 bp. Matepair sequencing also identified genes that were truncated by the breakpoints.

Genotyping, cloning and sequencing.

Genotyping of polymorphic loci and amplification of all breakpoint junctions by long-range PCR and DNA sequencing were performed as described in (Bonaglia MC et al. 2009). Target sequences for quantitative PCR (qPCR) analysis were selected using the Primer Express 3.0 software (Applied Biosystems); qPCR assays were performed on an ABI PRISM 7900HT sequence detection system (Applied Biosystems). Long-range PCRs were performed with JumpStart Red ACCUTaq LA DNA polymerase (Sigma) and the following protocol: 30 sec at 96°C, 35 cycles of 15 sec at 94°C/ 20 sec at 58°C/ 15 min at 68°C, 15 min final elongation time. Sequencing reactions were performed with a Big Dye Terminator Cycle Sequencing kit 3.1 (Life Technologies) and run on an ABI Prism 3500AV Genetic Analyzer.

4. Results

We collected data from conventional and molecular karyotypes (Tabel 1, 2, 3), parental origin of the deleted and duplicated fragments (Table 4) and breakpoint characterization (Table 5).
FISH analysis with specific subtelomeric probes was used to confirmed the *de novo* origin of each rearrangement.
The subject of our study were divided into four different classes, A, B, C and D, thanks to the data derived from array-CGH analysis that allowed us to discover the size of each rearranged regions.

4.1 Class A: classical unbalanced translocations

In class A are grouped 29 subjects for which the analysis showed a classical unbalanced translocation, with a terminally deleted chromosome on which the terminal portion from a donor chromosome has been transposed. Data derived from conventional karyotype, array-CGH analysis and the size of the deleted and duplicated regions are listed in Table 1. Additional details are provided below for case 25 and 26.

Case 25

Conventional karyotype analysis of case 25 revealed three different cell lines. The main cell line, which represented the 78% of the cells, showed a wild type male karyotype (Figure 1). A second line with an unbalanced translocation t(9;14)(q11;p11) was found in 20% of the metaphases analysed (Figure 2,3), and the minor one with a chromosome 9 trisomy was found in 2% of the cells (Figure 4). The percentages were established on 100 blood metaphases and further confirmed by FISH on 250 interphase nuclei using chromosome 9 and 14 painting probes. We were unable to define whether the derivative chromosome is a der(14) or a der(9) (Figure 3,5).

A 180K CGH+SNP array (Agilent) and a 500K SNPs (Illumina) genotyping microarray showed the presence of a 46,XY karyotype without any trace of the unbalanced lines.

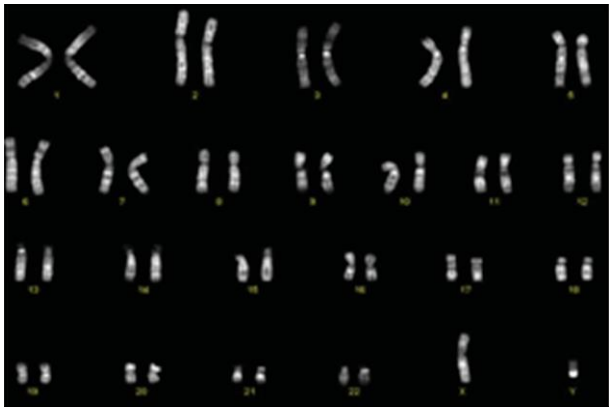

Fig. 1 46,XY Q-banding karyotype showing the cell line with normal karyotype

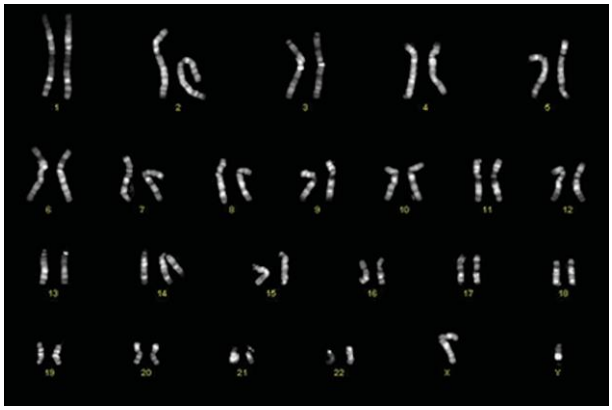

Fig. 2 Karyotype analysis showing a derivative chromosome

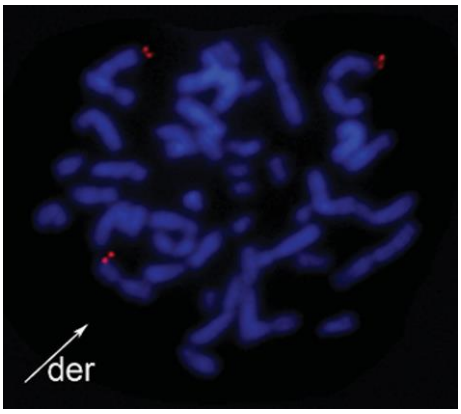

Fig. 3 FISH with the 9q34 LS1ABL probe (red) confirming the derivative chromosome (arrow)

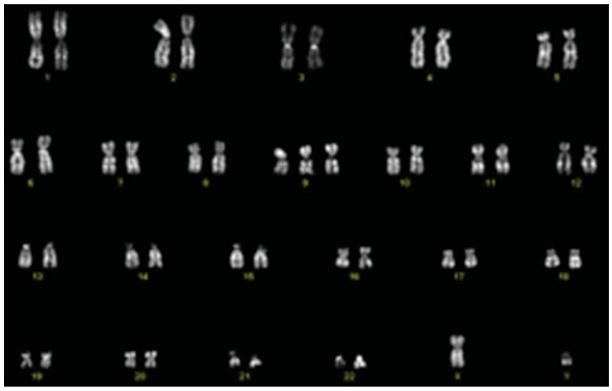

Fig. 4 Q-banding karyotype showing 47,XY,+9 in 2% of metaphase cells analysed

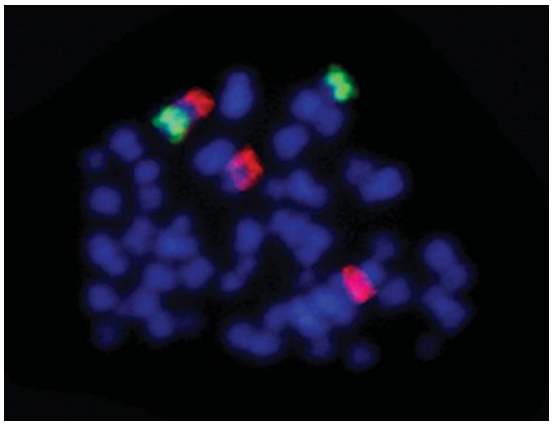

Fig.5 FISH with whole chromosome 9 (red) and 14 (green) probes

Case 26

The analysis of case 26 showed two cell lines identified by conventional karyotype, FISH and array-CGH analysis.

Blood cells karyotype showed mosaic condition between a wild type female cell line and a cell line with an unbalanced translocation, where part of the long arm of the chromosome 14 was translocated to the distal q arm of chromosome 2.

FISH analysis on fibroblast metaphases with subtelomeric probes demonstrated the presence of a 2q deletion (Figure 6) in 100% of the cells and additional 14q material on the der(2) chromosome in 22% of the cells analysed (Figure 7).

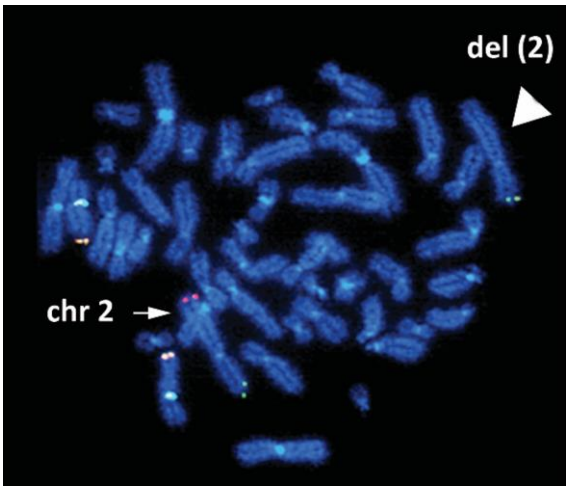

Fig. 6 FISH with subtelomeric 2p (aqua) and 2q probe (red, TelVysion, Vysis). Chromosome 2 with q arm deletion (arrowhead). Additional probes served as internal controls: telomeric Xq (yellow) and centromeric X chromsome (aqua).

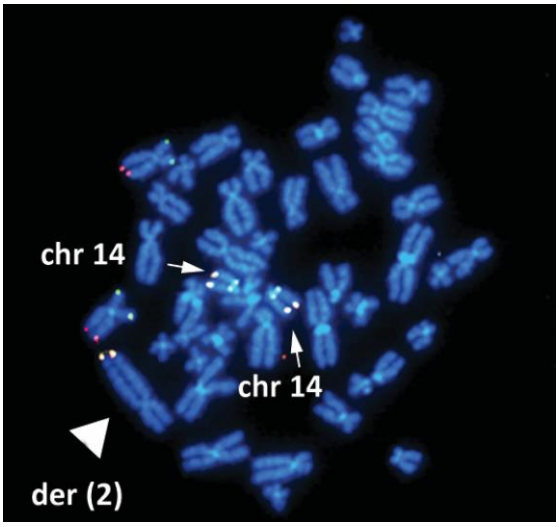

Fig. 7 FISH with a subtelomeric 14q probe (TelVysion, Vysis) shows signals only on the homologues chromosome 14 (arrow) and on the 2q chromosome (arrowhead). Additional probes served as internal controls: 14q11.1 (aqua), 7p (green) and 7q (red).

Array-CGH analysis confirmed the presence of an homogeneous 2q distal deletion, showing a chromosome 2 deletion in 100% of the DNA from both blood and fibroblasts (Figure 8, 9). However, only 70% (log ratio: +0.44) of the DNA extracted from blood cells showed the 14q duplication, while the analysis did reveal any duplication in the DNA extracted from fibroblasts, probably due to the resolution threshold for the detection of a mosaicisms (Figure 10, 11).

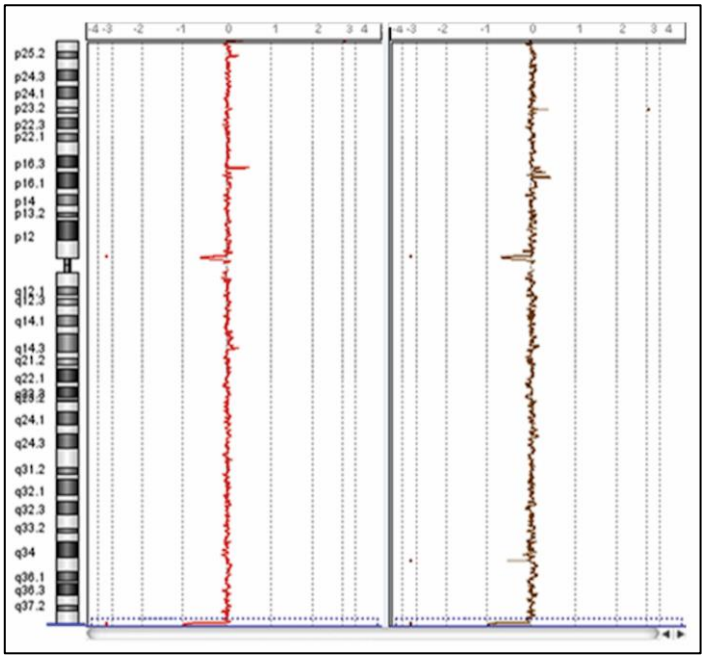

Fig. 8 Array-CGH profile of whole chromosome 2 showing a terminal deletion at 2q in blood (left) and fibroblast (right).

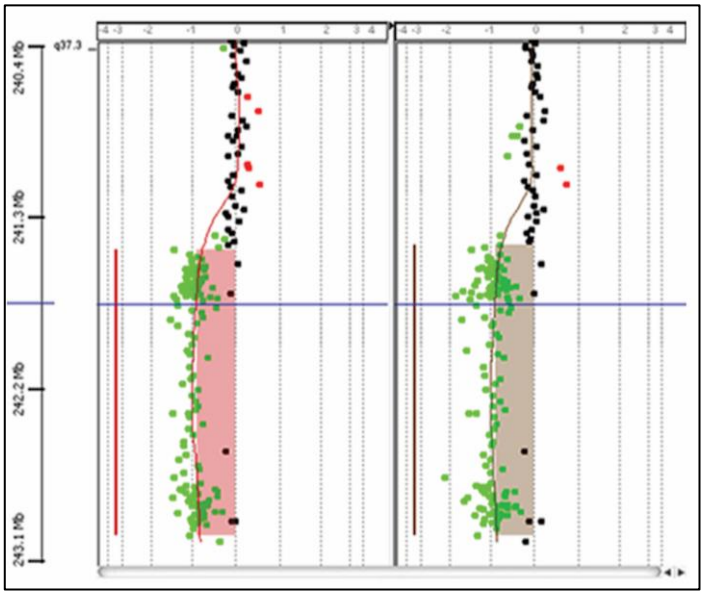

Fig. 9 An enlargement of the array-CGH profile for the 2q37.3 deletion of ~1.5 Mb detected both in blood (left) and fibroblasts (right).

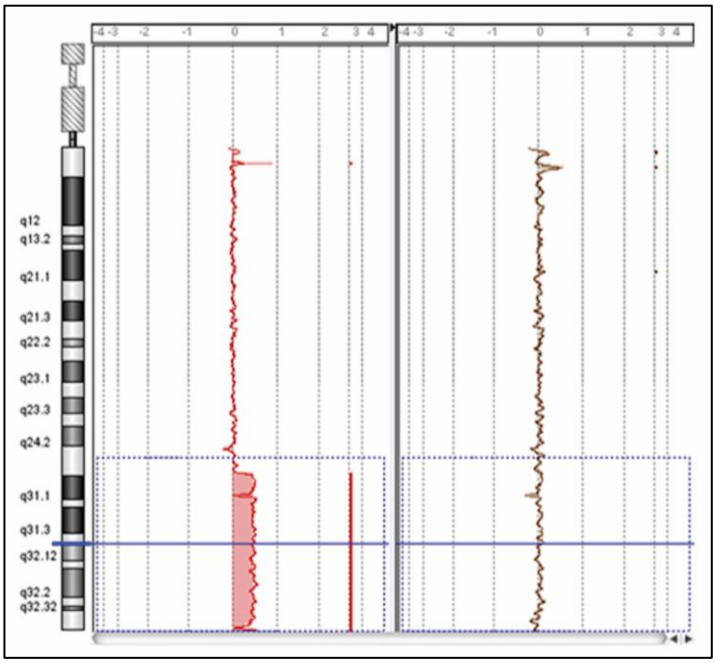

Fig.10 Array-CGH profile of whole chromosome 14 showing mosaic 14q24.3q32.3 duplication detected in blood (left) and a normal profile in fibroblasts (right).

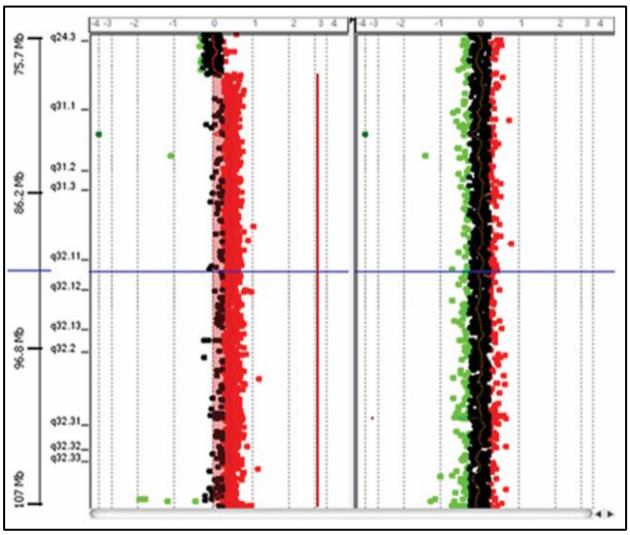

Fig. 11 An enlargement of the array-CGH profile 14q24.3q32.3 duplication detected in blood (left) and a normal profile in fibroblasts (right).

FISH analysis using the PAN-Tel probe showed hybridization signals on the telomeric long arm of both chromosomes 2 in all the 100 fibroblasts we analysed (Figure 12). Therefore, case 26 carries a terminal 2q deletion repaired by telomere healing in part of the cells and by the telomere capture of a 29 Mb portion of chromosome 14q in the others.

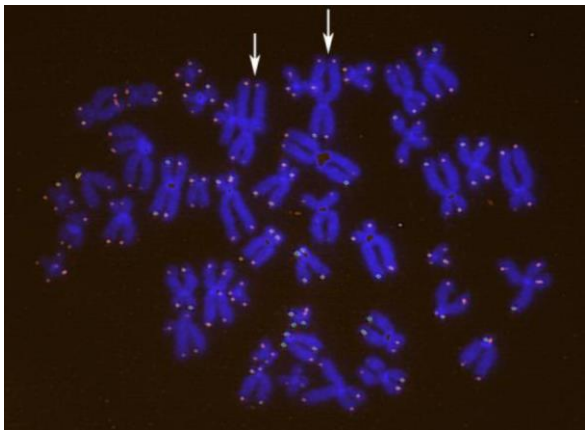

Fig. 12 An enlargement of the array-CGH profile 14q24.3q32.3 duplication detected in blood (left) and a normal profile in fibroblasts (right).

Table1: array-CGH result and conventional karyotype description of simple unbalanced translocation cases

Case n.	Subject ID	Array-CGH result	Karyotype	Deletion size	Duplication size
1	BP7202	arr[hg19] 8p23.3p22(161,472-13,558,082)x3(13,604,086) x2; 9p24.3p24.2(204,193-4,566,061)x1(4,576,878x2)	46,XY,der(9)t(8;9)(p22;p24.2)	4.6 Mb	13.5 Mb
2	BP4008	arr[hg19] 3q28q29(188,607,686)x2(188,885,872-197,807,677)x3; 13q33.2q34(105,833,932)x2(106,068,058-115,058,961)x1	46,XY,der(13)t(3;13)(q28;q33.2)	8.9 Mb	8.9 Mb
3	BP27506	arr[hg19] 17q24.2q25.3(64,612,454)x2(64,635,007-81,099,040)x3; 18q23 (76,176,614)x2(76,194,150-78,010,032)x1	46,XY,der(18)t(17;18)(q24.2;q23)	1.8 Mb	16.5 Mb
4	BP15808	arr[hg19] 4p16.3p15.2(45,882-22,302,368)x3(22,327,409)x2); 10p15.3p15.1(136,361-5,327,281)x1(5,337,021)x2	46,XY,der(10)t(4;10)(p15.2;p15.1)	5.3 Mb	22.0 Mb
5	BP23104	arr[hg19] 9p24.3p24.2(204,193-4,428,633)x1(4,454,773)x2; 16q24.1q24.3 (84,272,586)x2(84,284,222-90,163,114)x3	46,XY,der(9)t(9;16)(p24.2;q24.1)	4.4 Mb	5.8 Mb
6	BP30910	arr[hg19] 8p23.3-p23.1(161,472-8,100,443)x3(8,111,027)x2; 8p23.1(9,883,009)x2(9,909,239-11,850,681)x3, 18q22.1-q23(64,494,120)x2(64,526,770-78,010,032)x1	46,XY,der(18)t(8;18)(p23.1;q22.1)	13.4 Mb	7.9 Mb/ 1.9 Mb
7	BP20010	arr[hg19] 13q33.3q34(108,071,157)x2(108,082,624-114,123,340)x1; Xq28(153,542,123)x2(153,555,953-154,886,057)x3	46,XY,der(13)t(13;X)(q33.3;q28)	6.0 Mb	1.3 Mb
8	BP62411	arr[hg19] 22q13.2q13.33(42,204,882)x2(42,218,960-51,186,249)x1; 20q13.33(61,758,593)x2(61,785,315-62,949,149)x3	46,XX,der(22)t(22;20)(q13.2;q13.33)	8.9 Mb	1.2 Mb
9	BP14380	arr[hg19] 1q43q44 (239,375,517)x2(239,412,361-249,212,668)x3; 13q33.3q34 (109,793,969)x2(109,804,708-115,105,297)x1	46,XX,der(13)t(1;13)(q43;q33.3)	5.3 Mb	9.8 Mb
10	PV8805	arr[hg19] 5p15.33p14.1(364,108-27,830,956)x1(28,393,916)x2; 10q25.1q26.3(107,522,856)x2(107,669,748-135,404,471)x3	46,XX,der(5)t(5;10)(p14.1;q25.1)	27.8 Mb	27.7 Mb
11	PV67208	arr[hg19] 5p15.33(26,142-1,159,917)x1(1,188,502)x2; 8p23.3p21.2(161,472-25,624,737)x3(25,641,243)x2	46,XY,der(5)t(5;8)(p15.33;p21.1)	1.1 Mb	25.5 Mb
12[§]	PV109808	arr[hg19] 1p36.33p36.32(564,424-3,472,959)x1(3,479,133)x2; 3p26.3p21.33(73,914-43,834,038)x3(43,865,299)x2	46,XX,der(1)t(1;3)(p36.32;p21.33)	2.9 Mb	43.8 Mb
13[◆]	PV68008	arr[hg19] 4q34.3q35.2(179,738,838)x2(179,819,307-190,916,678)x1; 6q16.1q27(98,882,071)x2(98,917,989-170,911,240)x3	46,XY,der(4)t(4 ;6)(q34.3;q16.1)	11.0 Mb	72.0 Mb
14	PV189908	arr[hg19] 4p16.316.1(45,882-6,558,998)x1(6,575,620)x2; 20q13.33(60,137,888)x2(60,145,660-62,949,149)x3	46,XY,der(4)t(4;20)(p16.1;q13.33)	6.5 Mb	2.8 Mb
15	PV189608	arr[hg19] 4p16.3(71,552-3,872,380)x1(4,190,047)x2; 7p22.3p22.1(42,976-6,870,943)x3(7,044,310)x2	46,XX,der(4)t(4;7)(p16.3;p22.1)	3.8 Mb	6.8 Mb

Case n.	Subject ID	Array CGH result	Karyotype	Deletion size	Duplication size
16	PV203708	arr[hg19] 19p13.3(259,395-930,809)x1(939,422)x2; 20p13p12.3(60,747-6,288,696)x3(6,317,254)x2	46,XX,der(19)t(19;20)(p13.3;p12.3)	0.6 Mb	6.2 Mb
17	PV142508	arr[hg19] 4q34.2q35.2(176,379,601)x2(176,391,701-190,916,678)x1; 20p13p12.1(67,778 -13,300,334)x3(13,329,904)x2	46,XX,der(4)t(4;20)(q34.2,p12.1)	14.5 Mb	13.2 Mb
18	PV124708	arr[hg19] 2q37.1q37.3(233,710,501)x2(233,722,638-243,041,364)x1; 9p24.3(204,193-1,101,466)x3(1,129,821)x2	46,XY,der(2)t(2;9)(q37.1;p24.3)	9.3 Mb	0.9 Mb
19	M8313	arr[hg19] 16q11.2 q24(46,500,741-90,163,070)x3; Xq28(149,105,821-155,196,740)x1	46,XX,der(X)t(16;X)(q11.2;q28)	6.0 Mb	43.6 Mb
20	M5412	arr[hg19]9p24.2p22.1(204,193-19,080,660)x1; 17q25.2q25.3(74,801,652-81,098,985)x3	46,XY,der(9)t(9;17)(p22.1;q25.2)	18.9 Mb	6.3 Mb
21	PV62106	arr[hg19] 1q42.11q44(224,069,954)x2(224,210,564-249,212,609)x3; 2q35q37.3(220,515,496)x2(220,691,174-243,102,476)x1	46,XY,der(2),t(1;2)(q42.11;q35)	22.4 Mb	25.0 Mb
22	PV21413	arr[hg19] 6q27(169,011,336-170,911,181)x1;19p13.3(266,117-2,613,231)x3	46,XX,der(6)t(6;19)(q27;p13.3)	1.9 Mb	2.3 Mb
23	BP14142	arr[hg19] 8p23.3p23.2(161,472-4,693,738)x1(4,704,674)x2; 9p24.3p24.2(204,193-4,051,530)x3(4,065,626)x2	46,XX,der(8)t(8;9)(p23.2;p24.2)	4.5 Mb	3.8 Mb
24	FIB556	arr[hg19] Xp22.33(61,329-1,957,875)x1;Yp11.3(11,091-1,785,694)x1; Xq28(153,238,318-153,406,374)x2; Xq28(154,120,538-154,841,596)x2	46,XY,der(Y)t(X;Y)(q28;p11.3)	1.7 Mb	0.1 Mb/ 0.7 Mb
25	PV43214	arr[hg19](1-22)x2(XY)x1	46,XY[78]/47,XY,+9[2]/46,XY,der (14?) or (9?)t(9;14)(q11;p11)[20]		
26	PV45914	arr[hg19] 2q37.3(241,591,565-243,087,697)x1; 14q24.3q32.33(78,504,178-107,287,446)x2≈3	46,XX,del(2)[70]/46,XXder(2) t(2,14)(q37.3;q24.3)[50]^ 46,XX,del(2)[78]/46,XXder(2) (t2,14)(q37.3;q24.3)[22]^^	1.5 Mb	28.7 Mb
27	BP41507	arr 13q33.3q34(108,942,275)x2(109,299,357-115,058,961)x1; 18q21.31q23(53,876,613)x2(54,037,167-77,917,359)x3	46,XY,der(13)t(13;18)(q33.3;q21.31)	5.7 Mb	23.8 Mb
28	BP64715	arr 1q43q44(243,666,674)x2(243,684,045-249,212,668)x1; 3q29(194,119,246)x2(194,130,086-197,845,254)x3	46,XX,der(1)t(1;3)(q43;q29)	5.5 Mb	3.7 Mb
29	BP1653	arr 7q35q36.3 (146,981,087)x2(146,997,284-159,118,566)x3; 9p24.3p23(204,19312,114,297)x1(12,163,230)x2	46,XX,der(9)t(7;9)(q35;p24)	12.1 Mb	12.1 Mb

• : chorionic villi
§ : amniotic fluid
^ : blood cells
^^ : fibroblasts

4.2 Class B: inv-dup del translocations

In class B are grouped 7 subjects for which conventional karyotype and array-CGH analysis revealed a derivative chromosome with a distal deletion and an apparently contiguous duplication of the same chromosome, to which a distal portion of another chromosome was translocated. A short normal copy number region, corresponding to the fold-back portion of the truncated chromosome during formation of the dicentric chromosome, was detected between deletion and duplication in most inv-dup del rearrangements (Zuffardi O et al. 2009).

The duplicated fragment has been analysed by dual-colour FISH and breakpoint cloning, showing that it was a inverted duplication, thus, the rearranged chromosome carries an inverted duplication deletion (inv-dup del) on which a segment of the donor chromosome has been attached.

Data derived from conventional karyotype, array-CGH analysis and the size of the deleted and duplicated regions are listed in Table 2.

Case 30:

Abuelo et al. analysed case 30 by FISH analysis, with a subtelomeric Xp probe, proving a *de novo* unbalanced Xp;5q translocation with distal Xp deletion and distal 5q duplication of ~20 Mb (Abuelo DN et al. 2000). Subsequently the array-CGH analysis confirm the presence of the 5q duplication and the Xp deletion already identified, and revealed a 2 Mb Xp terminal duplication.

The Xp duplication has been analysed by dual-colour FISH on interphase nuclei (Figure 13) showing the presence of an inverted Xp22.33-p22.32 duplication (red-green-green-signal, Figure 13, RIGHT). Therefore, the final interpretation of the rearrangement was 46,XX,der(X)t(inv-dup delX;5)(p22.3;q34) (Table 2).

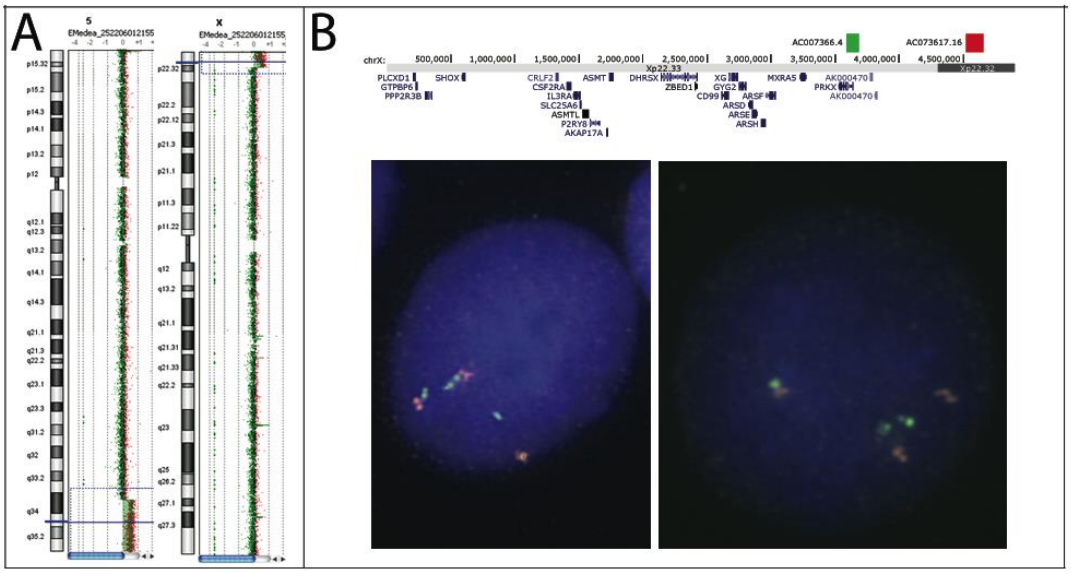

Fig. 13 A: array-CGH profile of the chromosomes 5 and X involved in the translocation, showing the 5q34q35.3 duplicated region of ~20Mb (left profile) and the Xp22.33p22.32 duplication of ~2 Mb (right profile). B: FISH analysis to test the orientation of the duplicated Xp22.33-p22.3 segment. UCSC map (hg19) and probes used (AC007366, green) and (AC073617, red) (top), dual-colour interphase FISH (bottom).

Case 31

Aldred et al analysed case 31 by conventional karyotype, dual-colour FISH and STS marker analysis classifying it as a inverted-duplication deletion (2q) (case 63 from Aldred MA et al. 2004).

We re-analysed the case by high-resolution array-CGH (kit 244K, Agilent) to better characterize the interval between duplicated and deleted regions. Our analysis detected the presence of 2q36.3q37.3 duplicated region and a deletion on distal chromosome 2q, furthermore revealed an additional duplication of the terminal portion of chromosome 1p36.33p36.32, indicating that the rearrangement was not a classical inv-dup del but a translocation t(inv-dup del2;1)(q26.3;p36.32) (Table2, Figure 14).

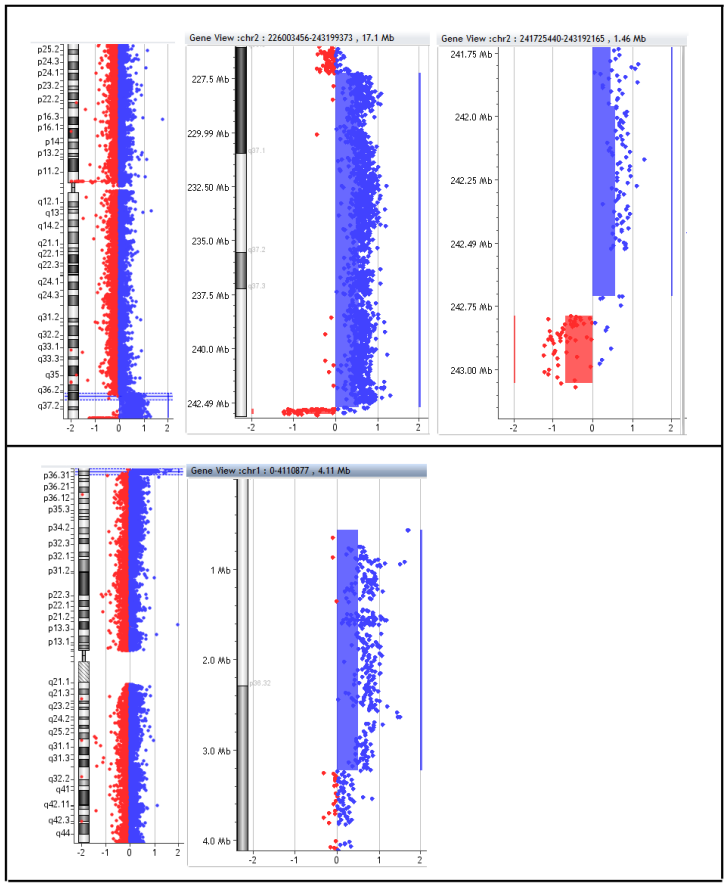

Fig. 14 UP: array-CGH profile of whole chromosome 2 (left) and magnified view of array plot showing the 2q duplicated region contiguous to the distal 2q deletion. BOTTOM: array-CGH profile of whole chromosome 1 (left) and magnified view of array plot showing the 1p duplicated region

Case 32

Conventional karyotype and subtelomeric FISH analysis was used to detected a derivative 16p+ chromosome (Figure 13). Array-CGH analysis detected a terminal 5p duplication, a terminal 16p deletion, and a proximal 16p duplication, with a normal copy region between the 16p deletion and duplication (Figure 15, 23). The final interpretation of the rearrangement was 46,XX,der(16)t(5;16)(p15.1;p13.3) (Table 2).

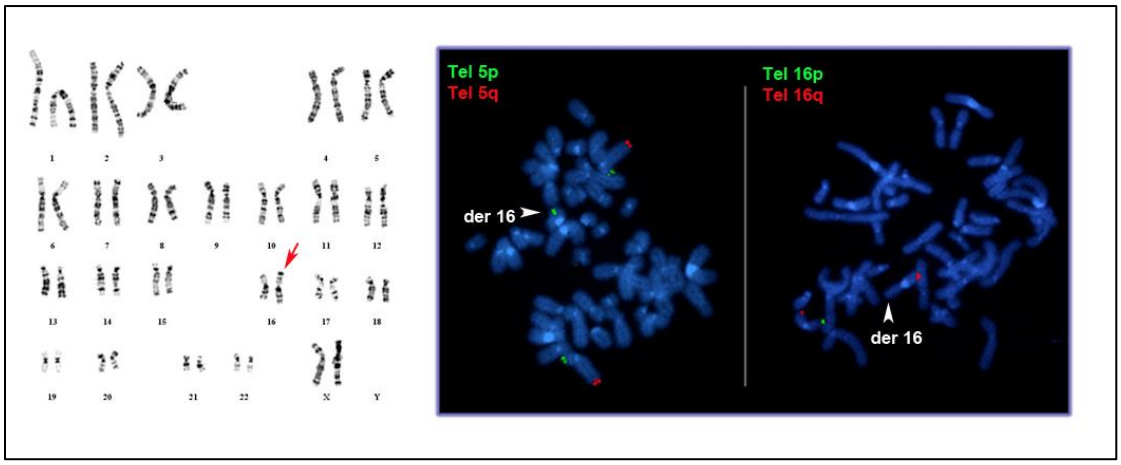

Fig. 15 LEFT: G-banding karyotype showing an abnormal chromosome 16p+ (red arrow). RIGHT: FISH analysis with 5p and 16p subtelomeric probes (Tel Vysion, Vysis) showing the derivative chromosome 16 (arrow).

Case 33

Conventional karyotype showed an unbalanced translocation with a distal chromosome 7q duplication. Array-CGH and dual-colour FISH analysis detected that the duplication region was inverted and revealed the presence of a 63.5 Kb 7q terminal deletion (Table2). Furthermore, the analysis

showed that the satellite of the short arm of a D/G group chromosome repaired the broken chromosome. A specific low copy repeats take part to the mechanism mediating this type of translocation, and its role has been already discussed (Beri S et al. 2013).

Case 34, case 35, case 36

Conventional karyotype and subtelomeric FISH analysis was used to detected a derivative 8p+ chromosome in case 34, 35 and 36 (Figure 16). Subsequently Array-CGH analysis showed the terminal 8p deletion of 6.9 Mb (case 34 and 36) and 7.7 Mb (case 35), and revealed an additional proximal 8p duplication and a normal copy region between the deleted and duplicated fragments in all subjects. The array-CGH analysis confirmed the presence of the 17p13.2 (4.1 Mb) duplication in case 34, the Xq28 (3.9 Mb) terminal duplication in case 35 and 6q28 terminal duplication (8.1 Mb) in case 36 (Table 2, Figure 16). Moreover, the 8p duplication region has been analysed by dual-colour FISH on interphase nuclei showing the presence of an inverted duplication Therefore, the final interpretation of the rearrangement was 46,XX,der(8)t(invdup8;17)(p23.1;p13.2) in case 34, 46,XY,der(8)t(invdup8;X)(p23.1;q28) in case 35 and 46,XX,der(8)t(invdup8 ;6)(p23.1 ;q26) in case 36 (Table 2).

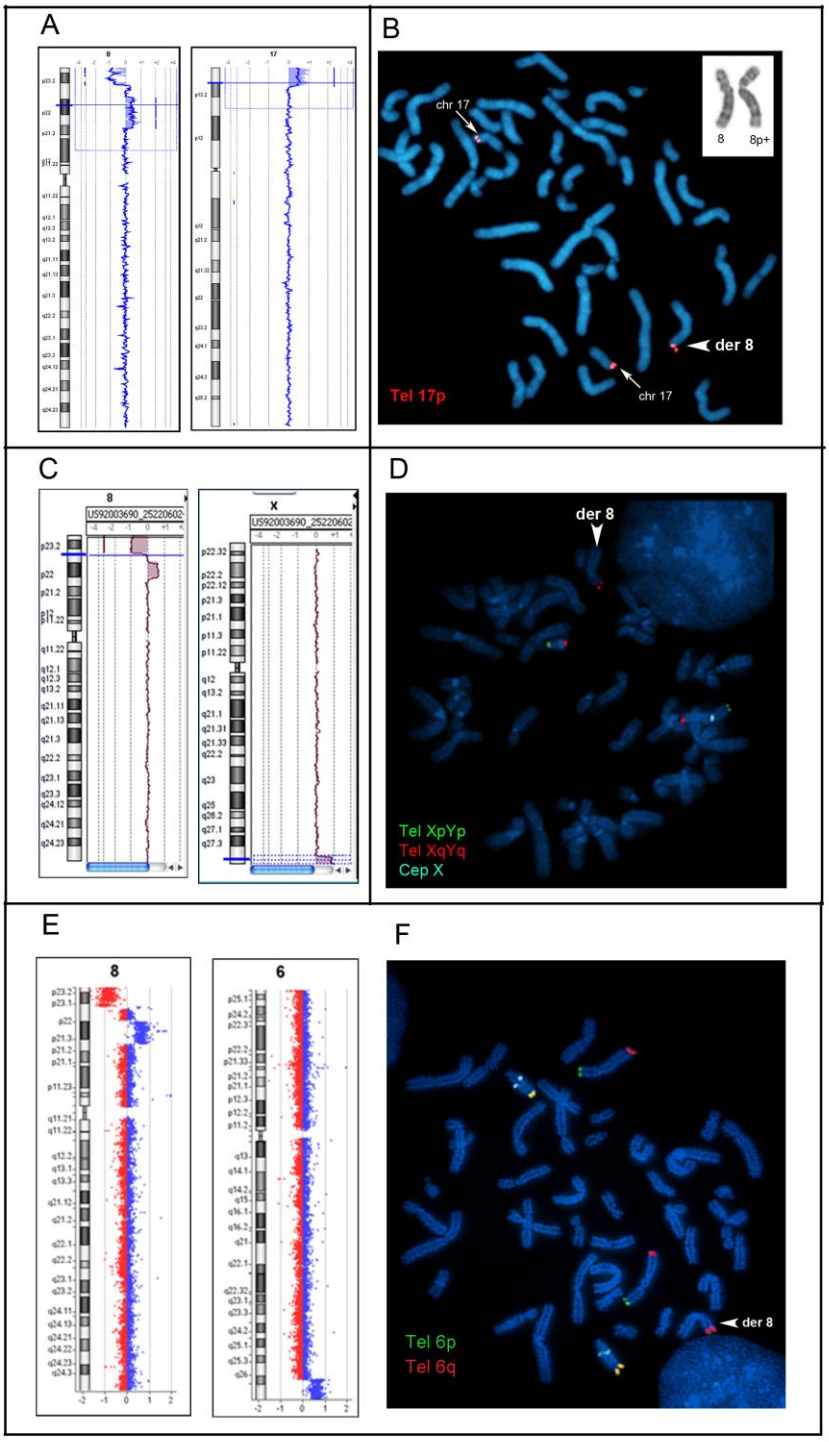
A
B
chr 17
8
8p+
der 8
Tel 17p
chr 17
C
8
X
D
der 8
Tel XpYp
Tel XqYq
Cep X
E
8
6
F
der 8
Tel 6p
Tel 6q

Fig. 16 A, C, E: array-CGH profile of the chromosomes 8 (left) showing the deleted and duplicated 8p terminal regions. The array profile on the left shows a distal 17p13.3p13.2 duplication in case 34 (**A**), the Xq28 duplication in case 35 (**C**) and a 6q26q27 duplication in case 36 (E).
profile) and the Xp22.33p22.32 duplication of ~2 Mb (right profile). **B**: Subtelomeric FISH probe (Cytocell), labelled in red, for the p-arm of chromosome 17 (arrow) shows hybridisation to the p-arm of derivative chromosome 8 (arrowhead). In the upper right corner, a G-banding cut-out of chromosomes 8 showing an abnormal chromosome 8p+ is presented. **D**: FISH analysis with the subtelomeric XY probe mix (Vysis) containing: XpYp probe (green), XqYq probe (red) and CEP X (aqua). The analysis shows a red signal on the derivative chromosome 8 (arrowhead) in addition to the signals on both arms of chromosome X. **F**: FISH analysis with the subtelomeric 6 probe mix (Vysis) containing: 6p probe (green), 6q probe (red), 13q (yellow) and LSI 13 (13q14, aqua). The analysis shows a red signal on the derivative chromosome 8 (arrowhead) in addition to the signals on both arms of chromosome 6.

4.3 CLASS C: simple unbalanced inversions

In 6 subjects, grouped in class C, the analysis showed derivative chromosomes that mimicked the recombinants of parental pericentric inversions (Table 3, Figure 21). FISH analysis with specific subtelomeric probes was used to confirmed that in all cases the deleted chromosome acquired the distal portion of its opposite arm (Figure 17, 18).

Data derived from conventional karyotype, array-CGH analysis and the size of the deleted and duplicated regions are listed in Table 3. Additional details are provided below for cases 41 and 42.

Table 2: array-CGH result and conventional karyotype description of inv-dup del translocation cases

Case n.	Subject ID	Array-CGH result	Karyotype	Deletion size	Duplication size
30*	BP52607	arr[hg19]5q34q35.3(162,108,625)x2(162,150,936-180,905,260)x3; Xp22.33p22.32 (61091-61,588)x1(179,680-4,995,869)x3(5,028,348)x2	46,XX,der(X)t(invdupX;5)(p22.32;q34)	61.5 Mb	4.8 Mb
31*	BP53208	arr[hg19]1p36.33p36.32(564,405-3,224,201)x3(3,235,900)x2; 2q36.3q37.3(227,248,961)x2(227,256,501-242,744,540)x3 (242,788,731-243,068,343)x1	46,XX,der(2)t(invdup2;1)(q36.3;p36.32)	0.3 Mb	chr1: 3.2 Mb/ chr2:15.5 Mb
32	PV86802	arr[hg19]5p15.33p15.1(26,142-17,192,364)x3(17,200,450x2); 16p13.3(106,271-1,125,151)x1(1,138,590-1,206,981)x2 (1,217,496-2,100,490)x3(2,109,963)x2	46,XX,der(16)t(invdup16;5)(p13.3;p15.1)	1.1 Mb	chr5: 17.0 Mb/ chr16: 0.9 Mb
33*	BP8398	arr[hg19]7q35q36.3(144,063,347)x2(144,093,894-158,612,902)x3 (158,721,577)x2;7q36.3(158,747,771-158,811,268)x1	46,XX,der(7)t(invdup7;satDoG)(q35; satDoG)	0.6 Mb	14.5 Mb
34	PV52608	arr[hg19]8p23.3p21.2(191,530-6,914,026)x1(7,302,590-12,241,093)x2 (12,583,259-24,493,086)x3(24,773,595)x2;17p13.3-p13.2(84,287-4,192,663)x3(4,221,088)x2	46,XX,der(8)t(invdup8;17)(p23.1;p13.2)	6.9 Mb	chr8:12.0 Mb/ chr17:4.1 Mb
35	FIB629	arr[hg19]8p23.3p21.3(176,814-7,786,708)x1(8,100,384-11,764,412)x2 (11,796,358-19,051,664)x3(19,087,267)x2;Xq28(151,198,447-155,190,224)x2	46,XY,der(8)t(invdup8;X)(p23.1;q28)	7.7 Mb	chr8: 7.2 Mb/ chrX:3.9 Mb
36	BP78615	arr 6q26q27(162,777,193-170,911,240)x3; 8p23.3(176,814-6,939,296)x1; 8p23.1p21.3(11,906,207-20,531,706)x3	46,XX,der(8)t(invdup8 ;6)(p23.1 ;q26)	6.9 Mb	chr6: 8.1 Mb/ chr8: 8.6 Mb

*: Case 30 (Abuelo et al. 2000), Case 31 (Aldred MA et al.2004), Case 33 (Beri S et al.2013)

Case 41

Conventional karyotype and array-CGH analysis detected a derivative X chromosome with a terminal Xp11.4 duplication of 40.5 Mb and a distal Xq26.1 deletion of 25.5 Mb (Table 3). FISH analysis with specific subtelomeric probes showed that the Xp duplicated fragment was translocate on the distal q arm of the same chromosome (Figure 17). Thus, the final interpretation of the karyotype was 46,XX,der(X)dup(X)(p11.4)del(X)(q26.1) (Table 3).

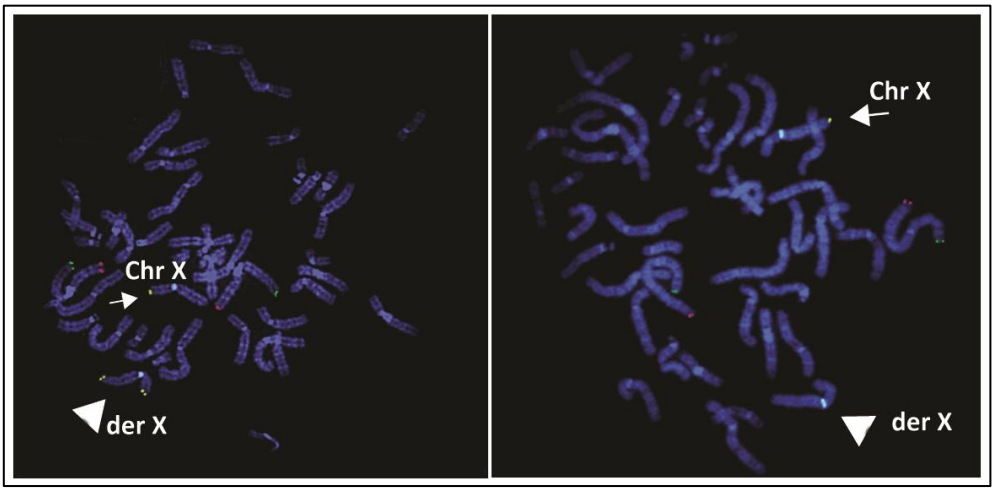

Fig. 17 LEFT: FISH analysis with subtelomeric Xp probe (yellow, Tel Vysion, Vysis) shows signals on the p-arm of the normal chromosome X (arrow) and on both arms of the derivative chromosome X (arrowhead). The probe mix also contains a second set of subtelomeric probes used as internal controls: 2p (spectrum green), 2q (red) and CEP X (aqua). RIGHT: FISH analysis with subtelomeric Xq probe (yellow, TelVysion, Vysis) shows signals on the q-arm of the normal chromosome X (arrow) and no signals of the derivative chromosome X (arrowhead). Additional subtelomeric probes used as internal controls: 1p (green), 1q (spectrum red) and CEP X (aqua).

Case 42:

Conventional karyotype analysis detected a derivative 9 chromosome and array-CGH analysis confirmed a 9p22.3 duplication of 16.7 Mb and a distal 9q34.3 deletion of 32.8 Mb (Table 3). FISH analysis with specific subtelomeric probes showed that the 9p duplicated fragment was translocated on the distal q arm of the same chromosome (Figure 18).

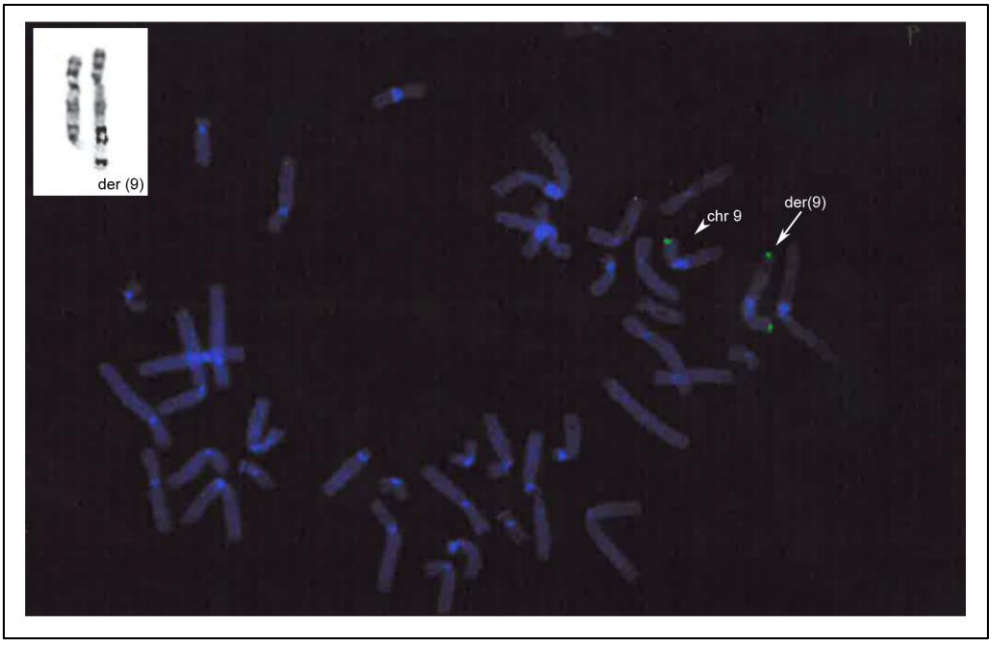

Fig. 18 FISH analysis with subtelomeric probe (green, Q-Biogene) shows signals on the p-arm of the normal chromosome 9 (arrowhead) and on both arms of the derivative chromosome 9 (arrow). In the upper left corner a G-banding cut-out of chromosomes 9 is presented showing the der(9).

Table 3: array-CGH result and conventional karyotype description of simple and inverted-duplication deletion unbalanced inversion cases

Case n.	Subject ID	Array-CGH result	Karyotype	Deletion size	Duplication size
37[§]	PV130708	arr[hg19] Xp22.1(1,592,583-41,701,000x3;41,726,000)x2; Xq21.33q28(96,477,151)x2(96,489,837-154,582,414)x1	46,XX,der(X)dup(X)(p22.1)del(X)q(21.33)	58.0 Mb	40.1 Mb
38	BP13433	arr[hg19] 18p11.32p11.21(131,700-14,951,330)x1(14,966,006)x2; 18q22.1-q23(65,398,745)x2(65,398,745-78,010,032)x3	46,XY,der(18)del(18)(p11.21)dup(18)(q22.1)	14.9 Mb	12.6 Mb
39[*]	PV160310	arr[hg19] 2p25.3p25.1(30,341-9,588,369)x3; 2q37.2q37.3(235,744,424-243,041,305)x1	46,XY,der(2)dup(2)(p25.1)del(2)(q37.2)	9.6 Mb	7.3 Mb
40	PV15812	arr[hg19] 9p24.3p24.1(204,193-5,864,904)x1(5,881,429)x2; 9q34.11q34.3(132,315,993)x2(132,326,351-141,018,925)x3	46,XY,der(9)del(9)(p24.1)dup(9)(q34.11)	5.9 Mb	8.7 Mb
41	BP1560	arr[hg19] Xp22.33p11.4(154,121-40,506,366)x3(40,522,107)x2; Xq26.1q28(129,651,300)x2(129,681,455-155,232,907)x1	46,XX,der(X)dup(X)(p11.4)del(X)(q26.1)	25.5 Mb	40.5 Mb
42	INGM2141	arr[hg19] 9p24.3p22.3(220,253-16,526,609)x3(16,834,952)x2; 9q34.3(140,986,162-141,025,921)x1	46,XX,der(9)dup(9)(p22.3)del(9)(q34.3)	32.8 Mb	16.7 Mb
43	INGM2952	arr[hg19] 4p16.3(71,552-919,291)x1; 4p16.3p15.33(927,780-12,595,138)x3; 4q35.1q35.2(183,574,006-190,884,350)x3	46,XX,der(4)invdup(4)(p15.33)dup(4)(q35)	0.9 Mb	chr4p: 11.6 Mb/ chr4q: 7.3 Mb

§ : amniotic fluid
*: from Vetro A et al. 2014

4.4 CLASS D: inv-dup del unbalanced inversions

Case 43 was the only one case representing the Class D, relative to the inverted-duplication deletion unbalanced inversions. Conventional karyotype and array-CGH analysis showed a derivative chromosome 4 with a 4p16.3 distal deletion of 900 Kb contiguous to a proximal 4p16.3p15.33 duplication of 11.6 Mb, to which the terminal 4q35.1q35.2 was attached, leading to a 4q duplication of 7.3 Mb (Table 3, Figure 19, 23).

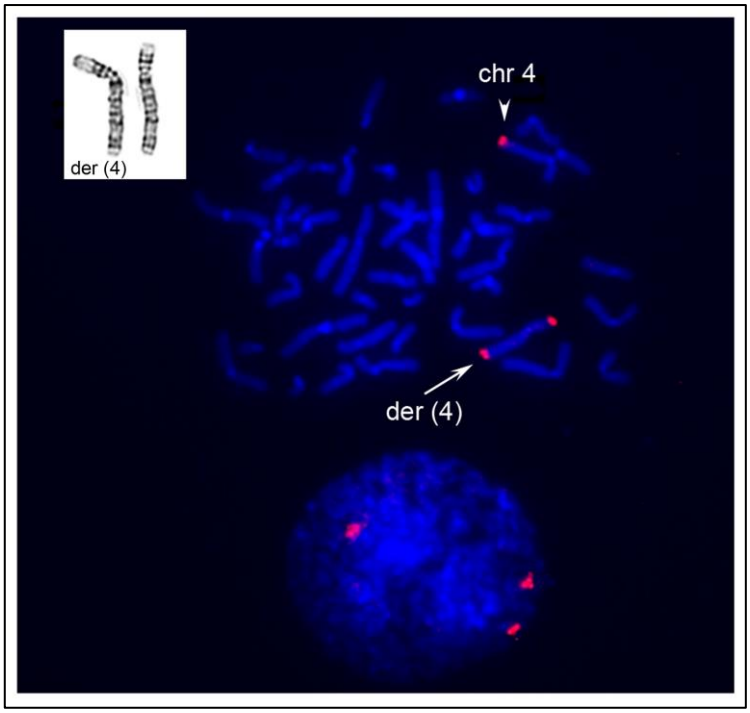

Fig. 19 FISH analysis with subtelomeric 4q probe (red, Kreatech) shows signals on the q-arm of the normal chromosome 4 (arrowhead) and on both arms of the derivative chromosome 4 (arrow). In the upper left corner a G-banding cut-out of chromosomes 4 is presented showing the der(4).

4.5 Parental origin

Parental origin analysis determined the origin of both the deleted and the duplicated regions in 27 cases (20 class A, 3 class B and 4 class C), in 9 cases we obtained a partial characterization (6 classA, 1 class B,C and D), whereas in 7 cases the analysis was not performed (3 class A, B, 1 class C) (Table 4). Most of the rearrangements, 24 out of 27, showed a uni-parental origin of the deleted and the duplicated fragments. In cases 7, 8, 14 and 42 only the origin of the deleted segment could be verified, while in cases 16, 21, 22, 33 and 43 only the duplicated segment was informative.

In cases 10 and 12, two classical unbalanced translocation cases grouped in class A, the analysis showed a bi-parental origin of the rearrangement and detected a paternal origin of the deletion and a maternal origin of the duplication. Moreover, case 9 (class A rearrangement), showed two maternal alleles in its duplicated portion. All cases grouped in class C simple unbalanced inversions we could analyse presented a paternal origin of their deleted and duplicated fragments (Table 4).

Table 4: parental origin of the 43 *de novo* unbalanced translocation/inversions cases

Case n.	Deletion origin	Duplication origin	Maternal/Paternal Age
1	Pat	Pat	32/32
2	Mat	Mat	34/37
3	Pat	Pat	25/36
4	Mat	Mat	42/52
5	Mat	Mat	23/25
6	Mat	Mat	33/-
7	Mat	U	24/31
8	Mat	U	37/38
9	Mat	Mat (3 alleles)	27/36
10	Pat	Mat	
11	Mat	Mat	
12	Pat	Mat	
13	Mat	Mat	
14	Mat	U	
15	Mat	Mat	
16	U	Pat	
17	Mat	Mat	
18	Pat	Pat	
19	Mat	Mat	35/40
20	Pat	Pat	31/30
21	U	Pat	
22	U	Pat	27/31
23	Mat	Mat	31/31
24	NT	NT	
25	NT	NT	
26	Pat	Pat	36/36
27	Mat	Mat	
28	NT	NT	
29	Mat	Mat	
30	NT	NT	
31	Pat	Pat	
32	NT	NT	
33	U	Pat	
34	Mat	Mat	
35	NT	NT	
36	Mat	Mat	
37	Pat	Pat	
38	NT	NT	22/-
39	Pat	Pat	37/40
40	Pat	Pat	37/36
41	Pat	Pat	17/23
42	Pat	U	53/56
43	U	Pat	34/36

Mat: maternal
Pat: paternal
U : uninformative ;
NT : not tested, not enough DNA or parental sample not available

4.6 Breakpoint analysis

Data obtained from breakpoint junction sequencing and breakpoint intervals determined by array-CGH analysis revealed that in 24 cases the breakpoint junctions interrupted a gene, preferentially on the recipient chromosome (20 out of 24 cases), in seven cases (cases 14, 22, 23, 28, 37, 42, 19 43) a gene interruption was observed at both deletion and duplication breakpoints, while in three class A cases (cases 7, 9 and 27) the breakpoints disrupt the *MYO16* gene on chromosome at 13q33.3 (Table 5).

Breakpoint junctions were cloned in 18 out of 43 cases, in particular: 12 classical unbalanced translocations (class A), 4 inv-dup del translocations (class B), 1 simple unbalanced inversion (class C) and the inv-dup del unbalanced inversion case. We characterized a total of 19 breakpoints, including those defining the junction between recipient and donor chromosome and the inv-dup del rearrangements (Table 5, Figure 18).

The analysis of the deletions/duplications junctions of class A detected several different sequences (Table 5, Figure 20). Case 2 showed NAHR between two LINE family 1 repeats, L1PA3 on chr 3 and L1H5 on chr 13, while in case 27 the breakpoint of the donor chromosome falls within a LINE repeat. Cases 6, 7, 12 and 23 carry micro-homologies sequences from 2 to 6 bases. Insertions from to 38 bases were detected in six cases: 3, 5, 8, 9, 18 and 28.

The breakpoint analysis of class B rearrangements also show a variety of breakpoint sequences (Table 5, Figure 20). In the junction between the inverted-duplicated chromosome X and duplicated chromosome 5 were present LINE sequences (LIPA2 and LIPA4) responsible for NAHR, while case 31 reveals a 3-bp microhomology.

In case 32, the breakpoint analysis of the junction between the normal and the inverted-duplication of chromosome 16 showed that a 19-base sequence of unknown origin is inserted at the breakpoint. While in the junction between chromosome 16 inverted duplication and chromosome 5 duplication in case 32 and between the inv-dup del 8p and chromosome 6 in case 36, a 4-base microhomology was present.

The junction of class C rearrangements could be determined in only in case 41, showing a 3- bp microhomology (Table 5, Figure 20).

Finally, in case 43 of class D we cloned the junction between the inverted/duplicated 4p and the donor 4q. This junction sequence shows a structure with three breakpoints, a 18-base inversion and a 6-base insertion (Table 5, Figure 18).

We failed to amplify the breakpoint junctions in four cases (cases 4, 10 and 29 Class A and case 42 Class C) probably due to the presence of GC-rich sequences (case 29), large repeats (case 42) or possibly cryptic complexity regions that are hard to analyse even with NGS technology. In all remaining cases, insufficient DNA was available for the analysis.

Table 5: breakpoint characterization and features of breakpoint junctions for all 43 cases.

Case n.	Breakpoint interval	Donor chromosome breakpoint	Recipient chromosome breakpoint	Features at breakpoint junction	Mechanism
1	chr8: 13,558,082-13,604,086 chr9:4,566,061-4,576,878	intergenic	*SLC1A1*		
2	°chr3:188,740,129-188,740,271 °chr13:106,034,376-106,034,900	intergenic	*TPRG1*	NAHR between L1PA3 on chr 3 and L1H5 on chr 13	LINE mediated NAHR
3	°chr17:64,618,160-64,618,161 °chr18:76,189,456-76,189,457	intergenic	*PRKCA*	13-bp insertion; Alu on chr 17	NHEJ
4	°chr4: 22,300,261-22,303,501 °chr10: 5,324,691-5,328,434	intergenic	intergenic		
5	°chr9:4,434,505-4,434,506 °chr16:84,281,970-84,281,971	intergenic	intergenic	1-bp insertion; L2 on chr 9, L1 on chr 16	NHEJ
6	chr8: 8,100,443-8,111,027 chr8: 9,883,009-9,909,239 chr18:64,502,947-64,502,950	intergenic	intergenic	3-bp microhomology; L1 on chr.8	MMEJ
7	chr13:109,283,528-109,283,534 chrX:153,897,671-153,897,677	intergenic	*MYO16*	6-bp microhomology; LINE1 on chr.X	MMEJ
8	chr22:42,206,043-42,206,044 chr20:61,766,972-61,766,973	intergenic	*CCDC134*	36-bp insertion of MT DNA sequence	NHEJ
9	°chr1:239,391,222-239,391,223 °chr13:109,795,831-109,795,832	intergenic	*MYO16*	5-bp insertion; L1 on chr 1	NHEJ
10	°chr5:27,830,956-28,393,916 °chr10:107,522,856-107,669,748	intergenic	intergenic		
11	chr5:1,159,917-1,188,502 chr8:25,624,737-25,641,243	*PPP2R2A*	intergenic		
12	°chr1:3,480,538-3,480,540 °chr3:43,837,847-43,837,849	intergenic	*MEGF6*	2-bp microhomology; LTR16A on chr 3	MMEJ
13	chr4:179,738,838-179,819,307 chr6:98,882,071-98,917,989	intergenic	intergenic		
14	chr4:6,558,998-6,575,620 chr20:60,137,888-60,145,660	*CDH4*	*PPP2R2C*		
15	chr4:3,872,380-4,190,047 chr7:6,870,943-7,044,310	LCRs	LCRs		
16	chr19:930,809-939,422 chr20:6,288,696-6,317,254	intergenic	*ARID3A*		

Case n.	Breakpoint interval	Donor chromosome breakpoint	Recipient chromosome breakpoint	Features at breakpoint junction	Mechanism
17	chr4:176,379,601-176,391,701 chr20:13,300,334-13,329,904	*TASP1*	intergenic		
18	chr2:233,713,932-233,713,933 chr9:11,415,392-11,415,393	intergenic	*GIGYF2*	5-bp insertion; Alu on chr 2 and chr 9	NHEJ
19	chr16:46,447,079-46,500,741 chrX:149,084,932-149,105,821	LCRs	LCRs		
20	chr9:19,080,719-19,089,530 chr17:74,796,829-74,801,652	*LOC101928514*	*HUS6*		
21	chr1:224,069,954-224,210,564 chr2:220,515,496_220,691,174	LCRs	intergenic		
22	chr6:169,001,544-169,011,336 chr19:2,613,231-2,715,781	*GNG7*	*SMOC2*		
23	°chr8:4,695,484-4,695,488 °chr9:4,057,405-4,057,409	*GLISE*	*CSMD1*	4-bp microhomology	MMEJ
24	chrX:1,957,875- 1,977,345 chrY:1,785,694- 1,788,587 chrX: 153,234,144-153,238,318 chrX:153,406,374- 153,414,302 chrX:154,108,847-154,120,538 chrX:154,120,538-154,852,048				
25					
26	chr2:241,566,849-241,591,565 chr14:78465969-78,504,178	intergenic	*GPR35*		
27	chr13:109,270,366-109,270,367 chr18:53,984,381-53,984,382	intergenic	*MYO16*	Blunt-end ligation; LINE on chr13	NHEJ
28	chr1:243,670,896-243,670,897 chr3:194,128,080-194,128,081	*ATP13A3*	*AKT3*	3-bp insertion	NHEJ
29	chr7: 146,981,087-146,990,161 chr9: 12,114,297-12,136,147	*CNTNAP2*	intergenic		
30	BP1: 61,558-179,680 BP2:5,025557-5,025,608 chr5:162,139,723-162,139,774	intergenic	BP1: LCRs chrX BP2: intergenic	NAHR between LINE repeats on chr X and chr 5	LINE-mediated NAHR

Case n.	Breakpoint interval	Donor chromosome breakpoint	Recipient chromosome breakpoint	Features at breakpoint junction	Mechanism
31	BP1:227,253,790-227,253,793 BP2:242,744,540-242,788,731 chr1:3,226,830-3,226,833	LINE	BP1:intergenic	3-bp microhomology; LINE1 on chr.2	MMEJ
32	BP1:1,135,170-1,135,171 BP2:1,208,293-1,208,294 BP3:2,099,129-2,099,133 chr5:17,193,287-17,193,291	intergenic	BP1: intergenic BP2: *CACNA1H* BP3: *TCS2*	19-bp insertion at chr16/chr16 junction; 4-bp microhomology at chr16/chr15 junction	MMEH/NHEJ
33	BP1:144,063,347-144,093,894 BP3:158,721,577-158,747,771				
34	BP1:6,914,026-7,302,590 BP2:24,493,086-24,773,595 chr17:4,192,663-4,221,088	*UBE2G1*			
35	BP1:7,786,708-8,100,384 BP2:19,051,664-19,087,267 chrX:151182390-151,198,447	intergenic			
36	BP1:6,939,296-7,169,490 BP3:20,554,107-20,554,111 chr6:162,773,645-162,773,649	*PARK2*		4-bp microhomology	MMEJ
37	BP1:41,701,000-41,726,000 BP2:96,477,151-96,489,837	*DIAPH2*	*CASK*		
38	BP1:14,951,330-14,966,006 BP2:65,398,745-65,398,745	LCR	LCR		
39	BP1 :9,588,369-9,609,978 BP2:235646083-235,744,424	intergenic	*CPSF3*		
40	BP1:5,864,904-5,881,429 BP2:132,315,993-132,326,351	intergenic	intergenic		
41	°BP1:40,508,961-40,508,964 °BP2:129,668,386-129,668,389	intergenic	*MED14*	3-bp microhomology; ERV1 on chr Xq	MMEJ
42	BP1:16,705,259-16,722,823 BP2: 140,969,676-140,986,162	*BNC2*	*CACNA1B*		
43	°BP1:922,100-924,214 °BP2a:12,701,893-12,701,894 °BP2b:12,704,292-12,704,310 °BP3:183,568,492-183,568,493	BP1 : *GAK* BP2 :intergenic BP3 : intergenic	*TENM3*	FoSTeS: 6-bp insertion; L1PB1 on chr 4p and L1MB2 on chr 4q	FoSTeS

°: Breakpoint region suggested by Mate Pair Sequencing analys

Fig. 20 Sequence alignment of all cloned breakpoint junctions The nucleotide position, sequence alignment with the original chromosome sequences and repeat content of each case is shown. Homology and micro-homology regions are underlined. A drawing elucidating the structure of case 43 junction (Bottom).

Case 2

	Chr. Position (hg19)	Sequence
BP Dup/N	chr3:188740109-188740280	gtttccagtttttctgttctg.ttttttccccatctttgtggttttatctactttttggtctttgatgatggtgatgtacagatggg
Junction		TCAAAAagtttttctcgtctgttttttttccccatctttgtggttttatctactttttggtctttgatgatggtgatgtacagatggg
BP Del/N	chr13:106034355-106034527	TCAAAAagtttttctcgtctgttttttttccccatctttgtggttttatctactttttggtctttgatgatggtgatgtacagatggg

Sequence	Repeats
tttttggtgtggatgtcctttctgtttgttagttttccttctaacagacaggaccctcagctgcaggtctgttggagtaccctgcag	L1PA3, L1
tttttggtgtggatgtcctttctgtttgttagttttccttctaacagacaggaccctcagctgcaggtctgttggaataccctgctg	
tttttggtgtggatgtcctttctgtttgttagttttccttctaacagacaggaccctcagctgcaggtctgttggaataccctgctg	L1HS, L1

Case 3

	Chr. Position (hg19)	Sequence			Repeats
BP N/Dup	chr17:64618131-64618190	gcaacatagtgaaactccatccatttaaaa		acaacaacaacaaacagctagccatggcag	AluJr4, Alu
Junction		cttctcctcatcccagcctctcccatctgc	ctctcccatccca	acaacaacaacaaacagctagccatggcag	
BP Del/N	chr18:76189427-76189486	cttctcctcatcccagcctctcccatctgc		tcTGTGACCCAGGCCTTCAGCCTCAGTGTG	

Case 5

	Chr. Position (hg19)	Sequence			Repeats
BP Del/N	chr9:4434476-4434535 (rev compl)	cgtgctttgggtatctgctggtttccctgc		ctgagatgctattttctcattctccccaaa	L2c, L2
Junction		cgtgctttgggtatctgctggtttccctgc	a	tgtttttgggggctgatgacagtgttcagt	
BP N/Dup	chr16:84281941-84282000	acaggagcgggggttgggggctgggcatgt		tgtttttgggggctgatgacagtgttcagt	L1ME3A, L1

Case 6

	Chr. Position (hg19)	Sequence			Repeats
BP Del/N	chr18:64502918-64502980	TTAAATACTGAAAAAAAAAAAATACACCAG	AAT	CCCTGTTTTAAGGGAGCTGGAGGTTTATAT	
Junction		TTAAATACTGAAAAAAAAAAAATACACCAG	AAT	ttaagcaggttgatttttatagaagaaata	
BP N/Dup	chr8:9915965-9916027	taatccagattgaccccagaagaggtagaa	aat	ttaagcaggttgatttttatagaagaaata	L1MC4a, L1

Case 7

	Chr. Position (hg19)	Sequence			Repeats
BP Del/N	chr13:109283499-109283564	GCCTCTCGTGTTTTACTGCACTAGCAGAAT	GTCATT	ATTTTCCTTGCTGTGCCTCTGCAGAGGAAA	
Junction		GCCTCTCGTGTTTTACTGCACTAGCAGAAT	GTCATT	tagcccatttacatttaaggttaatattgt	
BP N/Dup	chrX:153897642-153897707	ccaatgtgccagtctgtgtcttttaattgg	gtcatt	tagcccatttacatttaaggttaatattgt	L1PA6, LINE

Case 8

	Chr. Position (hg19)	Sequence			Repeats
BP Del/N	chr22:42206014-42206073	GGCAGGGGGCAGCTCATGGCAGGTCCAGTC		TTTGATCTAGGCACTGATGGGTAAACAGGA	
Junction		GGCAGGGGGCAGCTCATGGCAGGTCCAGTC	ACCCCTTATCCCCATACTAGTTATTATCGAAACCAT	CAAGTCTTGGGGGCCTCTCTTGCTGCCAAG	
BP N/Dup	chr20:61766943-61767002	ggcggggcccagaggggcggTAGCCCCGC		CAAGTCTTGGGGGCCTCTCTTGCTGCCAAG	Simple rep.

Case 9

	Chr. Position (hg19)	Sequence			Repeats
BP N/Dup	chr1:239391193-239391252	tataaaggactacgattcagccataaaaag		aatcaggtgtgaatatatgatgaaggtgaa	L1MB7, L1
Junction		AACAAAATGGATAAGAGAAAATCATTAAAT	CATTA	aatcaggtgtgaatatatgatgaaggtgaa	
BP N/Dup	chr13:109795802-109795861	AACAAAATGGATAAGAGAAAATCATTAAAT		GAACAAATTAATATTTGCTTTTAGAACTAA	L1PA6, LINE

Case 12

	Chr. Position (hg19)	Sequence			Repeats
BP Del/N	chr1:3480509-3480570	GTCCTGCCAGGCCAGCCCCTCCTGGGCATA	GG	CACAAACAGCAACTGCTCGTTGTAAGGGAT	
Junction		GTCCTGCCAGGCCAGCCCCTCCTGGGCATA	gg	tgaggcctcttcctttggccaagggcagtt	
BP N/Dup	chr3:43837818-43837879	AAGATGCCCCAAGAATAGGGTATGACATTG	gg	tgaggcctcttcctttggccaagggcagtt	LTR16A, ERVL

Case 18

	Chr. Position (hg19)	Sequence			Repeats
BP Del/N	chr2:233713903-233713962	gtcactctgttgcccaagctggagtgcagt		agcgcgatctcagctcactgcaacctccaa	AluSx3, Alu
Junction		gtcactctgttgcccaagctggagtgcagt	gaacc	cgcctcccgggttcacgccattctcttgcc	
BP N/Dup	chr9:1141563-1141622 (rev compl)	agtggcacgatctcagctcactgcaagctc		cgcctcccgggttcacgccattctcttgcc	AluY, Alu

Case 23

	Chr. Position (hg19)	Sequence			Repeats
BP Del/N	chr8:4695456-4695518	TAGACACAATCTAGCAATGCTCACTGAGG	CATT	GCCTGTGAAGCCAGCAGGGGGCAGCAGCTC	
Junction		TGGATCCATCCCTAATAAAGATATCATAA	CATT	GCCTGTGAAGCCAGCAGGGGGCAGCAGCTC	
BP N/Dup	chr9:4057377-4057440	TGGATCCATCCCTAATAAAGATATCATAA	CATT	TTTATGCTAAAGAGCTTGATAGGAAAGCACA	

Case 27

	Chr. Position (hg19)	Sequence		Repeats
BP N/Dup	chr18:53984352-53984411	TTATTTTTTGTTAAATATTTAAGGGACCAA	TCATTGATATTTTCCCAAGAAAAAAGAGTC	
Junction		TCTCACTTCCCAATCCTGCCAGTCTTCAAG	TCATTGATATTTTCCCAAGAAAAAAGAGTC	
BP N/Del	chr13:109270337-109270396	TCTCACTTCCCAATCCTGCCAGTCTTCAAG	CTATTGCTTCCTGAGAATTTACCCAGTCTG	L2c, L2

Case 28

	Chr. Position (hg19)	Sequence			Repeats
BP Del/N	chr1:243670873-243670928	GTCGGAGCCTGTCAATGTACACAA		GTTAGTTCCTGCTGTGAGAGGCTGTGCATAGG	
Junction		GTCGGAGCCTGTCAATGTACACAA	TGT	AAATGCCTCATGATTTAAAAAGGCAAGTTAGC	
BP N/Dup	chr3:194128057-194128112	AGCTACATATTCTAATGTTACCCA		AAATGCCTCATGATTTAAAAAGGCAAGTTAGC	

Case 30

	Chr. Position (hg19)	Sequence	Repeats
BP Dup/N	chrX:5025543-5025627	aaaccactgctcaaggaaataaaagaggatacaaacaaatggaagaacattccatgctcatgggtacgaagaatcaatattgtga	LIPA2, LINE
Junction		aaaccactgctcaaggaaataaaagaggatacaaacaaatggaagaacattccatgctcatgggtaggaagaatcaatatcatga	
BP N/Dup	chr5:162139709-162139793	aaaccactgctcagtgaaataaaagaggatacaaacaaatggaagaacattccatgctcatgggtaggaagaatcaatatcatga	LIPA4, LINE

Case 31

	Chr. Position (hg19)	Sequence			Repeats
BP Dup/N	chr1:3226801-3226863	agatgacacctgCCCGGCACACTCTGGGGC	CCA	AAGGCCGGATGCCTGCAGTGTGCACACACC	
Junction		agatgacacctgCCCGGCACACTCTGGGGC	CCA	cctcactctaagacatcatcatctttatg	
BP N/Dup	chr2:227253761-227253823	tctttccatttctcactatttctacagtca	cca	cctcactctaagacatcatcatctttatg	L2, LINE

Case 32 - junction 1

	Chr. Position (hg19)	Sequence			Repeats
BP Del/Dup	chr16:1135141-1135200	CCTGCCAGGCCCTGCCCATGTGTTTCCTGA		GGGACACGGACGATGGTAGTGACCAGGCAG	
Junction		GCTGCCCCCACGGCTCCCCCAGCTCTTGGT	ATATATATATATATATGAC	GGGACACGGACGATGGTAGTGACCAGGCAG	
BP N/Dup	chr16:1208264-1208323 (rev comp)	GCTGCCCCCACGGCTCCCCCAGCTCTTGGT		GAGTGGGAAGGCCCCTCCCCCTGAGCCCTG	

Case 32 - junction 2

	Chr. Position (hg19)	Sequence			Repeats
BP Dup/N	chr5:17193258-17193321	gtggtgtgatctcagttcactgcagcctcc	gcct	cccgggttcaagaaattctcctgcctcagc	AluSx, Alu
Junction		gtggtgtgatctcagttcactgcagcctcc	gcct	aggcaacagagcaagactcagtctcaaaaa	
BP N/Dup	chr16:2099100-2099163 (rev comp)	agcgagcagagattgtgccactgcactcca	gcct	aggcaacagagcaagactcagtctcaaaaa	AluSx, Alu

Case 36

	Chr. Position (hg19)	Sequence			Repeats
BP Dup/N	chr8:20554082-20554135	AAAAGATTTTGGTCCAATTCCATCTT	AGGG	GATGGAAAGGGTTCCCTAAGATGG	
Junction		AAAAGATTTTGGTCCAATTCCATCTT	AGGG	CATGGATTAACAGATAAATAGTGA	
BP N/Dup	chr6:162773620-162773673	AGGGGAAAGCAATGGCATCACCCTGA	AGGG	CATGGATTAACAGATAAATAGTGA	

Case 41

	Chr. Position (hg19)	Sequence			Repeats
BP Del/N	chrX:40508935-40508994	AAAGAGGCAAAAGACATGATTTGTGAT	GAA	ACTTACTATTCAAATGCTAAATGTTTTCTG	
Junction		AAAGAGGCAAAAGACATGATTTGTGAT	GAA	GAACTCCATTTGGTGCTGGCCCAGGAGAGG	
BP N/Dup	chrX:129668360-129668419	GCCCAGGTACGAGGAAAAAGGGTAAAG	GAA	GAACTCCATTTGGTGCTGGCCCAGGAGAGG	

Case 43

	Chr. Position (hg19)	Sequence
BP1 Dup/N 4p	chr4:12701864-12701923	ATGTAAAATGATGGAAGTGGAGGAAGTTGC
BP2 Dup/N 4p	chr4:12704263-12704340 (rev compl)	agtcttttatccctcatccccctctcatgc
Junction		ATGTAAAATGATGGAAGTGGAGGAAGTTGC
BP3 Dup/N 4q	chr4:183568463-183568522	acagatttacaaaatgtttttatagtatga

Sequence			Repeats
		ATCAAACACCATTGACCACTGGAAGACTCC	
tttcccccaagtctccaa		agtccattgtatcactcctatgcctttgca	L1PB1, L1
tttcccccaagtctccaa	AGTTGC	aactaaaattctgtacctatcaaacaacaa	
		aactaaaattctgtacctatcaaacaacaa	L1MB2, L1

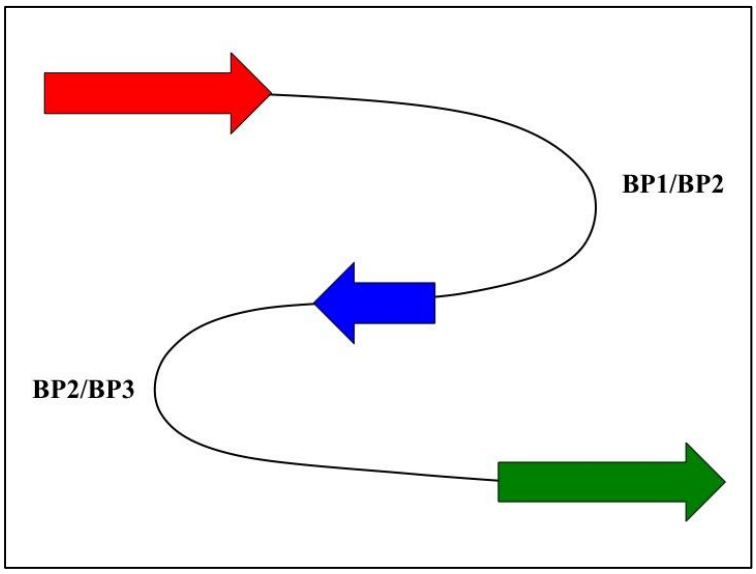

5. Discussion

We have studied 43 subjects with intellectual disability/psychomotor delay, couple infertility (case 25) and foetuses with congenital abnormalities, carriers of a *de novo* unbalanced rearrangements. Conventional karyotype, FISH, array-CGH, parental origin and breakpoint junctions analysis were systematically performed and allowed us to discriminate four different classes of rearrangements containing at least two imbalances on two different chromosomes (Classes A and B) or the opposite arms of the same chromosome (Classes C and D). In particular we dived them in: class A) simple translocations (n=29), class B) inverted-duplication deletion translocations (n=7), class C) simple inversions (n=6), class D) inverted-duplication deletion inversions (n=1). All subjects were sporadic cases, with the rearrangement present in all blood cells, except for two mosaic cases (cases 25 and 26) where at least one additional normal or abnormal cell line was detected

Class A and C rearrangements

Simple unbalanced translocations and inversions may originated from an undetected cryptic balanced tranlocations (class A) or balanced pericentric inversion (Class C) in mosaic, present in parents (Gijsbers AC et al. 2011). It is important to underline that mosaicism is a condition that can be likely masked by a high percentage of normal cells and its identification is related to the cell lines and the tissues examined, it is reasonable that mosaicism is not so rare as you think (Campbell IM et al. 2015).

However, this mechanism of origin presupposes the possible presence of brothers carriers the same rearrangements within the families, while no carrier siblings were found in our study. Furthermore, this type of imbalances could arise from a parental germinal mosaicism, but this type of apparently *de novo* rearrangements has always been reported in the literature as sporadic event, leading us to exclude this genesis hypothesis.

Our results suggested that simple unbalanced translocations and inversions can result from a terminal deletion subsequently stabilized by a telomerase-independent mechanism, through which the formation of a derivative chromosome is mediated by a telomere capture, involving another chromosome or the opposite arm of the same chromosome (Figure 21)(Flint J et al. 1994; Ballif BC et al. 2004).

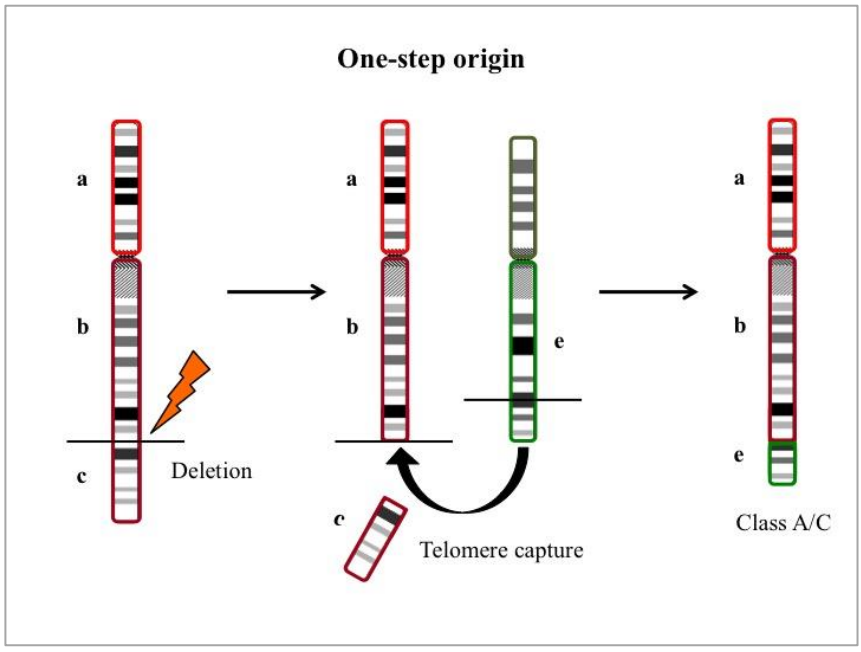

Fig. 21 Schematic representation of the one-step mechanisms of unbalanced translocations and unbalanced inversions showing a terminal chromosomal deletion healed by telomere capture.

We have analysed two mosaic cases that allow us to detect alternative mechanisms that could be responsible for class A and class C rearrangements. The analysis of case 26 showed the coexistence of a cell line carrying a distal 2q27.3 deletion, stabilized by the addition of (TTAGGG)n repeats, and a second line with a derivative chromosome 2 where a 14q24.3 duplicated region was translocated. Therefore, it is likely that the origin of the these rearrangements can be attributed to an initial terminal deletion subsequently repaired by two different repair mechanisms, telomere healing in the first cell line and telomere capture in the second line, that can act at in different cells leading to a mosaic condition.

The molecular characterization of case 25 showed the presence of three different cell lines: the main cell line with a normal karyotype, a second line with an unbalanced translocation t(9;14)(q11;p11) and a minor cell line with a chromosome 9 trisomy (Figure 22). The presence of the latter cell line and the advanced maternal age (40 years) are sufficient conditions to speculate that the origin of this rearrangement was a partial trisomy 9 rescue event. In particular, an initial trisomic zygote, probably due to a non-disjunction at maternal meiosis I (MI), underwent a trisomy rescue event in the early embryo generating a normal cell line and a cell line carrying the *de novo* unbalanced translocation. Thus, a partial trisomy rescue event originated the unbalanced cell line, with the elimination of 9p fragment and the stabilization of the 9q through the capture of a chromosome 14 (Figure 22).

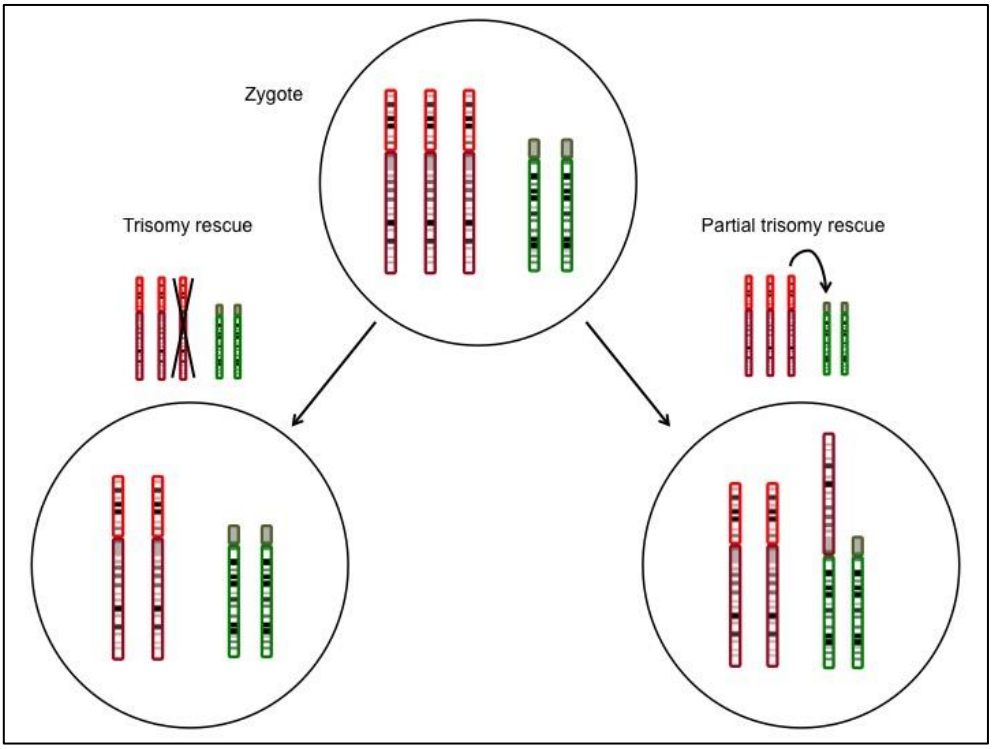

Fig. 22 Schematic representation of the events leading to the formation of the two cell lines in case 25. The zygote shows trisomy 9 (Top), subsequent to a non-disjunction event followed, post-zygotically, by a trisomy rescue event leading to a normal cell line (Bottom-left) and a partial trisomy rescue event (Bottom-right) leading to an abnormal cell line carrying an unbalanced translocation between the chromosome 9 and chromosome 14.

Considering these evidences we cannot exclude that in class A rearrangements, particularly those having a maternal origin of the duplication (15 out 20 class A cases), the unbalanced translocation reflects a partial rescue of a MI non-disjunction. Moreover, the fact that we detected three different alleles in only one duplication case (case 9) suggests that in most cases the non-disjunction takes place after the crossing-over.

According with this hypothesis Robberecht group estimated that 6 out their 12 cases of *de novo* unbalanced translocations originated at maternal meiosis I (Robberecht C et al. 2013). Furthermore, anaphase lagging of the

supernumerary chromosome and its shattering within the micronucleus may lead to the loss of a portion of the original chromosome that can be rescued through telomere capture as soon as it is reintegrated within the nucleus (Zhang CZ et al. 2015), while chromothripsis has already been described as a mutational mechanism for unbalanced translocations (Weckselblatt B et al. 2015). An alternative hypothesis for the genesis of class A and C rearrangements relies on the two-step mechanism, discussed in the next paragraph, driving the formation of class B and D rearrangements too.

Class B and D rearrangements

We collected 7 subject characterized by an inverted-duplication deletion translocation and one subject with an inverted-duplication deletion inversion, that have been rarely described in the literature (Fan YS and Siu VM 2001; Kostiner DR et al. 2002; Buysse K et al. 2009). These rearrangements are caused by three consecutive breakpoints that lead to the formation of a inverted-duplicated chromosome, through a mirror dicentric chromosome intermediate, and the subsequent telomere capture from another chromosome or the opposite arm of the same chromosome (Figure 23).

Dicentric chromosome are intrinsically unstable and prone to asymmetric breakage that generate a delete and a inverted-duplicated chromosomes (Zuffardi O et al. 2009), subsequently repaired by telomerase-mediated telomere healing or by telomere capture from another chromosome or the opposite arm of the same chromosome (Kostiner DR et al. 2002; Pham J et al. 2014).

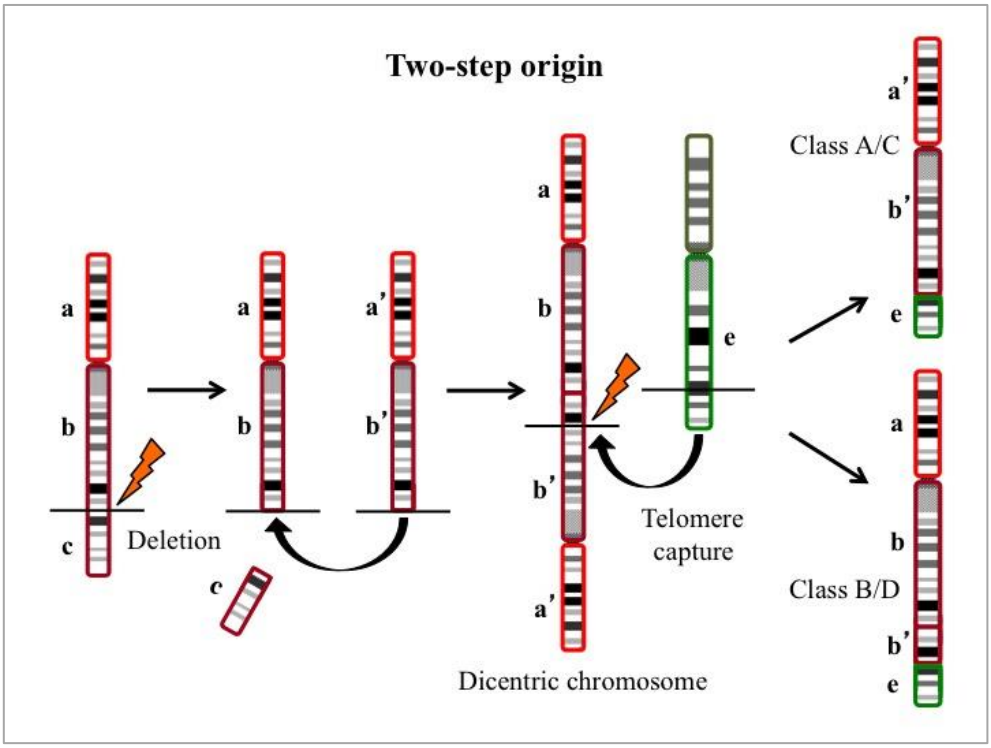

Fig. 23 Schematic representation of the two-step mechanisms of unbalanced translocations and unbalanced inversions showing how a terminal chromosomal deletion can be healed by telomere capture, subsequently to a dicentric-chromosome formation.

Segmental duplications, localized in 8p23, are involved in the formation of a dicentric chromosome 8 at maternal meiosis I by NAHR (Giglio S et al 2001), that once transmitted to the zygote it undergoes a series of breakage-fusion-bridge cycles in different cell during embryogenesis (Pramparo T et al. 2004). Then, the result of the selection constraints is that the only blood cell line detected postnatally carry the inv-dup del (8p).

According with these evidences we detected three cases with an inv-dup del (8p) translocation (case 34, 35 and 36) for which the multi-step origin is clear, with a first pre-zygotic event and the other(s) accourring post-zigotically.

Interestingly, the only case representing the class D rearrangements (case 43) demonstrates that these type of unbalanced inversions, apparently due to an unbalanced inversion associated with an inverted duplication, can be caused by a two-step event such as class B translocations cases (Figure 23).
Finally, it must be noted that the asymmetric breakage of a dicentric chromosome originates the inv-dup del chromosome and the complementary simply deleted chromosome. The latter might be responsible for the formation of the unbalanced translocations and inversions chromosomes grouped in class A and C (Figure 23).

Parental origin analysis

A maternal origin of both deleted and duplicated fragments was detected in the majority of the simple unbalanced translocations (class A), according to the results recently obtained from Robberecht and his group (Robberecht C et al. 2013). All class C rearrangements analysed showed a paternal origin of both unbalances, that could indicate that the dicentric chromosome, formed during paternal gametogenesis, have a higher likelihood to rearrange with itself, capturing the telomere on its opposite arm rather than another chromosome. Future large-scale parental origin studies of *de novo* unbalanced translocations/inversions will help to elucidate this point.
The finding that in two cases (case 10 and 12) the deleted and the duplicated fragments had biparental origin, without any mosaicim, suggest that the rearrangement is the result of two single temporally isolated events, with at least telomere capture occurring post-zygotically.

However, we cannot exclude that some of the initial rearrangements originated post-zygotically, as suggested by Robberecht and colleagues for up to 30-40% of all *de novo* unbalanced translocations (Robberecht C et al. 2013).

Breakpoint analysis

We successfully sequenced 19 breakpoints junctions from 18 unbalanced rearrangements, belonging to all subgroups, showing that the main mechanisms involved in the formation of unbalanced translocation and inversions are non-homologous end-joining and microhomology-mediated mechanisms such as MMEJ/MMBIR. Furthermore, case 43 showed more complex rearrangement with a18-base inversion and a 6-base insertion within the breakpoint junction, that can be explained by a Fork Stalling and Template Switching (FoSTes) event (Lee J et al. 2007), while in case 8 we detected a 36-base insertion identical to a mitochondrial DNA sequence, an occurrence already described in balanced translocations (Willett-Brozick JE et al. 2001).

Our findings do not confirm the hypothesis of Robberecht group, according to which NAHR, especially LINE-mediated, is the main mechanism leading to the unbalanced translocations, however validate the recent results obtained from Luo and Weckselblatt groups (Luo Y et al. 2011, Weckselblatt B et al. 2016).

Finally, in three cases (cases 7, 9, and 27) the breakpoint on the recipient chromosome disrupts the *MYO16* gene at 13q33.3 in three different positions, suggesting that this gene is a preferential target for NHEJ.

We were not able to determine the parental origin of the X chromosome duplication of case 7, but it is logical to assume that was inherited from the mother because the proband is a male. Therefore, according to the origin hypothesis of class A rearrangements, it is likely that the 13q deletion is the post-zigotyc event involved in the trisomy rescue mechanism.

Risk of recurrence

Our study suggest that *de novo* unbalanced translocations and inversions could originate by a single- or multi-step mechanisms acting at different developmental stages, pre- or post-zigatically. These findings thus indicate that there is no risk of recurrence of the rearrangement in a subsequent offspring, showing important implications for genetic counselling

References

Abuelo DN, Ahsanuddin AN, Mark HF. Distal 5q trisomy resulting from an X;5 translocation detected by chromosome painting. Am J Med Genet. 2000;94:392-399

Aldred MA, Sanford RO, Thomas NS, Barrow MA, Wilson LC, Brueton LA, Bonaglia MC, Hennekam RC, Eng C, Dennis NR, Trembath RC. Molecular analysis of 20 patients with 2q37.3 monosomy: definition of minimum deletion intervals for key phenotypes. J Med Genet. 2004;41:433-439.

Antonacci F, Kidd JM, Marques-Bonet T, Ventura M, Siswara P, Jiang Z, Eichler EE. Characterization of six human disease-associated inversion polymorphisms. Hum Mol Genet. 2009;18:2555-2566.

Ballif BC, Wakui K, Gajecka M, Shaffer LG. Translocation breakpoint mapping and sequence analysis in three monosomy 1p36 subjects with der(1)t(1;1)(p36;q44) suggest mechanisms for telomere capture in stabilizing de novo terminal rearrangements. Hum Genet. 2004;114:198-206.

Beri S, Bonaglia MC, Giorda R. Low-copy repeats at the human VIPR2 gene predispose to recurrent and nonrecurrent rearrangements. Eur J Hum Genet. 2013;21:757-761.

Bonaglia MC, Giorda R, Beri S, Bigoni S, Sensi A, Baroncini A, Capucci A, De Agostini C, Gwilliam R, Deloukas P, Dunham I, Zuffardi O. Mosaic 22q13 deletions: evidence for concurrent mosaic segmental isodisomy and gene conversion. Eur J Hum Genet. 2009;17:426-433.

Buysse K, Antonacci F, Callewaert B, Loeys B, Frankel U, Siu V, Mortier G, Speleman F, Menten B. Unusual 8p inverted duplication deletion with telomere capture from 8q. Eur J Med Genet. 2009;52:31-36.

Campbell IM, Shaw CA, Stankiewicz P, Lupski JR. Somatic mosaicism: implications for disease and transmission genetics. Trends Genet. 2015;31:382-392.

Chang YW, Wang PH, Li WH, Chen LC, Chang CM, Sung PL, Yang MJ, Cheng LY, Lai YL, Cheng YY, Yeh CC, Chang WH, Wang SY, Chen SR, Yen MS et al. Balanced and unbalanced reciprocal translocation: an overview of a 30-year experience in a single tertiary medical center in taiwan. J Chin Med Assoc. 2013;76:153-157

De Gregori M, Ciccone R, Magini P, Pramparo T, Gimelli S, Messa J, Novara F, Vetro A, Rossi E, Maraschio P, Bonaglia MC, Anichini C, Ferrero GB, Silengo M, Fazzi E, Maraschio P et al. Cryptic deletions are a common finding in "balanced" reciprocal and complex chromosome rearrangements: a study of 59 patients. J Med Genet. 2007;44:750-762.

Fan YS, Siu VM. Molecular cytogenetic characterization of a derivative chromosome 8 with an inverted duplication of 8p21.3-->p23.3 and a rearranged duplication of 8q24.13-->qter. Am J Med Genet. 2001;102:266-271.

Flint J, Craddock CF, Villegas A, Bentley DP, Williams HJ, Galanello R, Cao A, Wood WG, Ayyub H, Higgs DR. Healing of broken human chromosomes by the addition of telomeric repeats. Am J Hum Genet. 1994;55:505-512.

Gao M, Pang H, Zhao YH, Hua J, Tong D, Zhao H, Liu Y, Zhao Y, Zhang M, Yan XJ, Chen H, Ma HP, Jin TY, Dong SL. Karyotype analysis in large sample cases from shenyang women's and children's hospital: a study of 16,294 male infertility patients. Andrologia. 2016;11.doi: 10.1111/and.12649.

Giglio S, Broman KW, Matsumoto N, Calvari V, Gimelli G, Neumann T, Ohashi H, Voullaire L, Larizza D, Giorda R, Weber JL, Ledbetter DH, Zuffardi O. Olfactory receptor-gene clusters, genomic-inversion polymorphisms, and common chromosome rearrangements. Am J Hum Genet. 2001;68:874-883.

Gijsbers AC, Dauwerse JG, Bosch CA, Boon EM, Van Den Ende W, Kant SG, Hansson KM, Breuning MH, Bakker E, Ruivenkamp CA. Three new cases with a mosaicism involving a normal cell line and a cryptic unbalanced autosomal reciprocal translocation. Eur J Med Genet. 2011;54:409-412.

Giorda R, Bonaglia MC, Milani G, Baroncini A, Spada F, Beri S, Menozzi G, Rusconi M, Zuffardi O. Molecular and cytogenetic analysis of the spreading of X inactivation in a girl with microcephaly, mild dysmorphic features and t(X;5)(q22.1;q31.1). Eur J Hum Genet. 2008;16:897-905.

Jacobs PA, Browne C, Gregson N, Joyce C, White H. Estimates of the frequency of chromosome abnormalities detectable in unselected newborns using moderate levels of banding. J Med Genet. 1992;29:103-108.

Kato T1, Inagaki H, Tong M, Kogo H, Ohye T, Yamada K, Tsutsumi M, Emanuel BS, Kurahashi H. DNA secondary structure is influenced by genetic variation and alters susceptibility to de novo translocation. Mol Cytogenet. 2011;4:18.doi:10.1186/1755-8166-4-18.

Kleczkowska A, Fryns JP, Van den Berghe H. Pericentric inversions in man: personal experience and review of the literature. Hum Genet. 1987;75:333-338.

Kostiner DR, Nguyen H, Cox VA, Cotter PD. Stabilization of a terminal inversion duplication of 8p by telomere capture from 18q. Cytogenet Genome Res. 2002;98:9-12.

Lee J, Carvalho CM, Lupski JR. A DNA replication mechanism for generating nonrecurrent rearrangements associated with genomic disorders. Cell. 2007;131:1235-1247.

Luo Y, Hermetz KE, Jackson JM, Mulle JG, Dodd A, Tsuchiya KD, Ballif BC, Shaffer LG, Cody JD, Ledbetter DH, Martin CL, Rudd MK. Diverse mutational mechanisms cause pathogenic subtelomeric rearrangements. Hum Mol Genet. 2011;20:3769-3778.

Martin M. Cutadapt removes adapter sequences from high-throughput sequencing reads. EMBnet.Journal. 2011;17:10-12.

Pettenati MJ, Rao PN, Phelan MC, Grass F, Rao KW, Cosper P, Carroll AJ, Elder F, Smith JL, Higgins MD, Lanman JT, Higgins RR, Butler MG, Luthardt F, Keitges E et al. Paracentric inversions in humans: a review of 446 paracentric inversions with presentation of 120 new cases. Am J Med Genet. 1995;55:171-187.

Pham J, Shaw C, Pursley A, Hixson P, Sampath S, Roney E, Gambin T, Kang SH, Bi W, Lalani S, Bacino C, Lupski JR, Stankiewicz P, Patel A, Cheung SW. Somatic mosaicism detected by exon-targeted, high-resolution aCGH in 10,362 consecutive cases. Eur J Hum Genet. 2014;22:969-978.

Pramparo T, Giglio S, Gregato G, de Gregori M, Patricelli MG, Ciccone R, Scappaticci S, Mannino G, Lombardi C, Pirola B, Giorda R, Rocchi M, Zuffardi O. Inverted duplications: how many of them are mosaic?. Eur J Hum Genet. 2004;12:713-717.

Ravnan JB, Tepperberg JH, Papenhausen P, Lamb AN, Hedrick J, Eash D, Ledbetter DH, Martin CL. Subtelomere FISH analysis of 11 688 cases: an evaluation of the frequency and pattern of subtelomere rearrangements in individuals with developmental disabilities. J Med Genet. 2006;43:478-489.

Rivera H, Dominguez MG, Vasquez-Velasquez AI, Lurie IW. De novo dup p/del q or dup q/del p rearranged chromosomes: review of 104 cases of a distinct chromosomal mutation. Cytogenet Genome Res. 2013;141:58-63.

Robberecht C, Voet T, Zamani Esteki M, Nowakowska BA, Vermeesch JR. Nonallelic homologous recombination between retrotransposable elements is a driver of de novo unbalanced translocations. Genome Res. 2013;23:411-418.

Shao L, Shaw CA, Lu XY, Sahoo T, Bacino CA, Lalani SR, Stankiewicz P, Yatsenko SA, Li Y, Neill S, Pursley AN, Chinault AC, Patel A, Beaudet AL, Lupski JR et al. Identification of chromosome abnormalities in subtelomeric regions by microarray analysis: a study of 5,380 cases. Am J Med Genet. 2008;146:2242-2251.

Van Dyke DL, Weiss L, Roberson JR, Babu VR. The frequency and mutation rate of balanced autosomal rearrangements in man estimated from prenatal genetic studies for advanced maternal age. Am J Hum Genet. 1983;35:301-308.

Vetro A, Pagani S, Silengo M, Severino M, Bozzola E, Meazza C, Zuffardi O, Bozzola M. Severe growth hormone deficiency and pituitary malformation in a patient with chromosome 2p25 duplication and 2q37 deletion. Mol Cytogenet. 2014;7:41.eCollection

Warburton D. De novo balanced chromosome rearrangements and extra marker chromosomes identified at prenatal diagnosis: clinical significance and distribution of breakpoints. Am J Hum Genet. 1991;49:995-1013.

Weckselblatt B, Hermetz KE, Rudd MK. Unbalanced translocations arise from diverse mutational mechanisms including chromothripsis. Genome Res. 2015;25:937-947.

Willett-Brozick JE, Savul SA, Richey LE, Baysal BE. Germ line insertion of mtDNA at the breakpoint junction of a reciprocal constitutional translocation. Hum Genet. 2001;109:216-223.

Worsham MJ, Miller DA, Devries JM, Mitchell AR, Babu VR, Surli V, Weiss L, Van Dyke DL. A dicentric recombinant 9 derived from a paracentric inversion: phenotype, cytogenetics, and molecular analysis of centromeres. Am J Hum Genet. 1989;44:115-123.

Zhang CZ, Spektor A, Cornils H, Francis JM, Jackson EK, Liu S, Meyerson M, Pellman D. Chromothripsis from DNA damage in micronuclei. Nature. 2015;11:179-184.

Zuffardi O, Bonaglia M, Ciccone R, Giorda R. Inverted duplications deletions: underdiagnosed rearrangements??. Clin Genet. 2009;75:505-513.